# Microfacies of the Volgian-Ryazanian (Jurassic-Cretaceous) hydrocarbon seep carbonates from Sassenfjorden, central Spitsbergen, Svalbard

Krzysztof Hryniewicz, Øyvind Hammer, Hans A. Nakrem & Crispin T.S. Little

Hryniewicz, K., Hammer, Ø., Nakrem, H.A. & Little, C.T.S. Microfacies of the Volgian-Ryazanian (Jurassic-Cretaceous) hydrocarbon seep carbonates from Sassenfjorden, central Spitsbergen, Svalbard. *Norwegian Journal of Geology,* Vol 92, pp. 113-131. Trondheim 2012, ISSN 029-196X.

This paper presents a detailed analysis of microfacies of nine of the 15 hydrocarbon seep carbonates recorded from the Sassenfjorden area, Svalbard. These Late Volgian-latest Ryazanian carbonates have been found in the black shales of the uppermost Slottsmøya Member, Agardhfjellet Formation. The interval is characterised by a low sedimentation rate, which is testified by the presence of phosphatic grains and glaucony. Most of the carbonate formed within the sediment and is represented by two microfacies. Carbonate formation occurred mainly within the more permeable sediment pelletised by deposit feeders with micrite precipitating in the immediate surroundings. A difference in permeability caused localised fluid overpressure and episodes of hydrofracturing of calcareous mudstones, resulting in the localised occurrence of breccias. Surficial seep carbonates represent a variety of the microfacies, consisting of sponge boundstones and bioclastic sediments. These microfacies are relatively rare and mostly restricted to one or a few seeps and represent a spatial and temporal variation of surficial seep subenvironments, related perhaps to the type of substrate and fluid flow. Most of the seeps were relatively small and of short duration, which resulted from original sediment properties and perhaps from sealing of original fluid pathways by carbonate cementation. Only seep 9, developed in more permeable sediments, was larger and long-lasting. The prolonged duration of the seepage at this locality resulted in accumulation of a thick cover of bioclasts containing abundant microborings. These traces are made exclusively by chemoautotrophs and heterotrophs and indicate likely palaeodepths exceeding the depth of the photic zone during the latest Ryazanian. The stratigraphic distribution of microfacies indicates a change of original sediment from muds to more permeable silts and sands in the Late Ryazanian, which may be attributed to a shallowing episode.

*Krzysztof Hryniewicz, Øyvind Hammer, Hans A. Nakrem, Natural History Museum, P.O.Box 1172 Blindern, NO- 0318 Oslo, Norway. E-mail corresponding author: Krzysztof.Hryniewicz@nhm.uio.no Crispin T.S. Little, School of Earth and Environment, University of Leeds, Leeds LS2 9JT, United Kingdom.*

## Introduction

Ecosystems around submarine cold fluid emissions were first discovered in the deep marine environment at the Florida Escarpment (Paull et al. 1984), but continuous research has revealed that they are a relatively common phenomenon on passive, active and transform margins (e.g., Hovland 1992, Sibuet & Olu 1998, Levin 2005). Cold seeps are fueled by fluids with temperature either not exceeding or just slightly exceeding the average temperatures of bottom waters (Campbell 2006, Judd & Hovland 2007). Seeping fluids contain varying amounts of dissolved hydrocarbons of either biogenic or thermogenic origin (Martens et al. 1991, Sassen et al. 1999, cf. Judd & Hovland 2007). Seeping methane is utilised in the sediment by a consortium of anaerobic methane-oxidising archaea and sulphate-reducing bacteria through anaerobic oxidation of methane (Boetius et al. 2000, Valentine 2002, Reitner et al. 2005). In this reaction, precipitation of carbonate minerals and pyrite is facilitated at the expense of methane coming from shallow or deep sources and sea-water sulphate in pore waters. Sea-water sulphate is, therefore, essential for anaerobic oxidation of methane, and the rise of alkalinity and calcium carbonate precipitation at hydrocarbon seeps take place only in the surficial zone of the sediment where the sea-water sulphate has not yet been reduced (Naehr et al. 2000).

In the fossil record, carbonates precipitated in association with submarine hydrocarbon exhalations can be identified based on petrographical, geochemical or palaeontological evidence (e.g., Jørgensen 1976, Clari et al. 1988, Goedert et al. 2003, Kiel & Peckmann 2008, Peckmann et al. 2011, cf. Campbell 2006). In contrast to paleontology and geochemistry, relatively little is known about the sedimentary and earliest diagenetic processes shaping the morphology and anatomy of fossil seep carbonates. The relationships between fossil seep carbonates and faunas with the depositional environments in which they formed is also poorly studied. This state of the art is surprising since carbonates are susceptible to and record changes of the environment otherwise not recorded by clastic sedimentation. Microfacies analysis of limestones has proved to be a valuable tool in classical carbonate sedimentology (see Tucker & Wright 1990, Flügel 2004 for compilations), with application to reconstruction of, e.g., short-term changes in

palaeoenvironment (e.g., Gąsiewicz 1984, Strasser 1986), evolution of carbonate depositional environments (Wendt & Aigner 1985, Wendt & Belka 1991, Skompski & Szulczewski 1994), and biota and evolution of carbonate buildups (Flügel & Flügel-Kahler 1992, Monty et al. 1995 and references therein). The few examples of studies of sedimentological and earliest diagenetic processes at seep carbonates include studies on the spatial distribution of different types of carbonate and occurrence of coated grains in Late Cretaceous seeps on Hokkaido (Jenkins et al. 2007, 2008), description and interpretation of grapestone concretions from the Eocene of Bulgaria (De Boever et al. 2011), the anatomy and possible relations to gas hydrate in Miocene seeps from the northern Apennines (Conti & Fontana 2005, Dela Pierre et al. 2010), and reversed stromatactis structures described from the Oligocene Lincoln Creek seeps from Oregon (Peckmann et al. 2002).

In this paper we present a detailed description of the microfacies associated with sedimentation and early diagenesis, and an analysis of nine seep carbonate bodies from the Jurassic-Cretaceous transitional beds of Spitsbergen (Hammer et al. 2011). The aim of this analysis is to identify depositional and early diagenetic processes affecting seep carbonates during their formation in the shallow subsurface and on the sea floor. These processes can be identified from characteristic sedimentary structures, carbonate and non-carbonate grains, as well as biogenic structures. A detailed ammonite stratigraphy (Wierzbowski et al. 2011) provides a rare opportunity to analyse the Sassenfjorden seep carbonates in a stratigraphic context and to look at their evolution in relationship to the development of the depositional environment and the sedimentary basin.

## Geological setting

The Sassenfjorden hydrocarbon seeps comprise 15 small carbonate bodies cropping out along the southern coast of Sassenfjorden in central Spitsbergen, Svalbard archipelago (Fig.1). They all form small patches of heavily weathered and frost-wedged material with diameters not exceeding 2 m and a volume not greater than ≈ 6 $m^3$ each. Seep 9 is considerably larger and reaches 5 m in diameter and with a volume up to ≈ 20 $m^3$. Loose blocks with weathered surfaces allow observation of mesostructures and relations of some phases, but provide little information about the general shape and anatomy of the carbonate bodies. In addition to difficulties in defining the internal composition and shape of the carbonate bodies, screes covering an area of up to dozens of $m^2$ per seep and reaching up to 30 m downslope make it very difficult to identify the relationships of the seep carbonates to the enclosing rocks.

All of the seep carbonates are located 5 to 11 m below the top of the Slottsmøya Member of the uppermost Agardhfjellet Formation (Dypvik et al. 1991a, Hammer et al. 2011, Fig. 2). The youngest sediments of the Slottsmøya Member have traditionally been regarded as Volgian (Dypvik et al. 1991a, Nagy & Basov 1998). Recent investigations show that some of the seeps and therefore the top of the member are at least as young as the latest Ryazanian (Wierzbowski et al. 2011). The Slottsmøya Member is developed as black mudstones with sparse silty beds and dispersed carbonate concretions. It was deposited on an open shelf under oxygen-deficient conditions in a generally low-energy environment (Nagy et al. 1988, Dypvik et al. 1991b; Reolid et al. 2010) with the

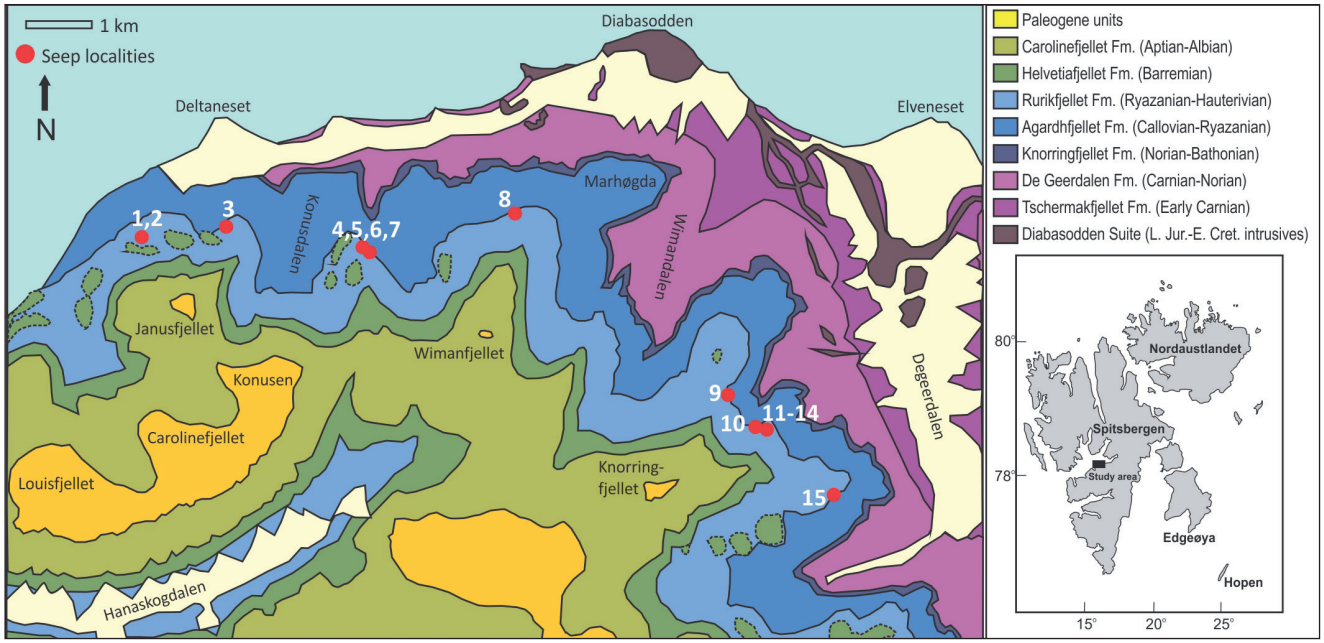


*Figure 1. Simplified geological map of the study area showing the locations of the seep carbonate bodies 1-15. Numbering from W to E. Modified from Dallmann et al. (2001).*

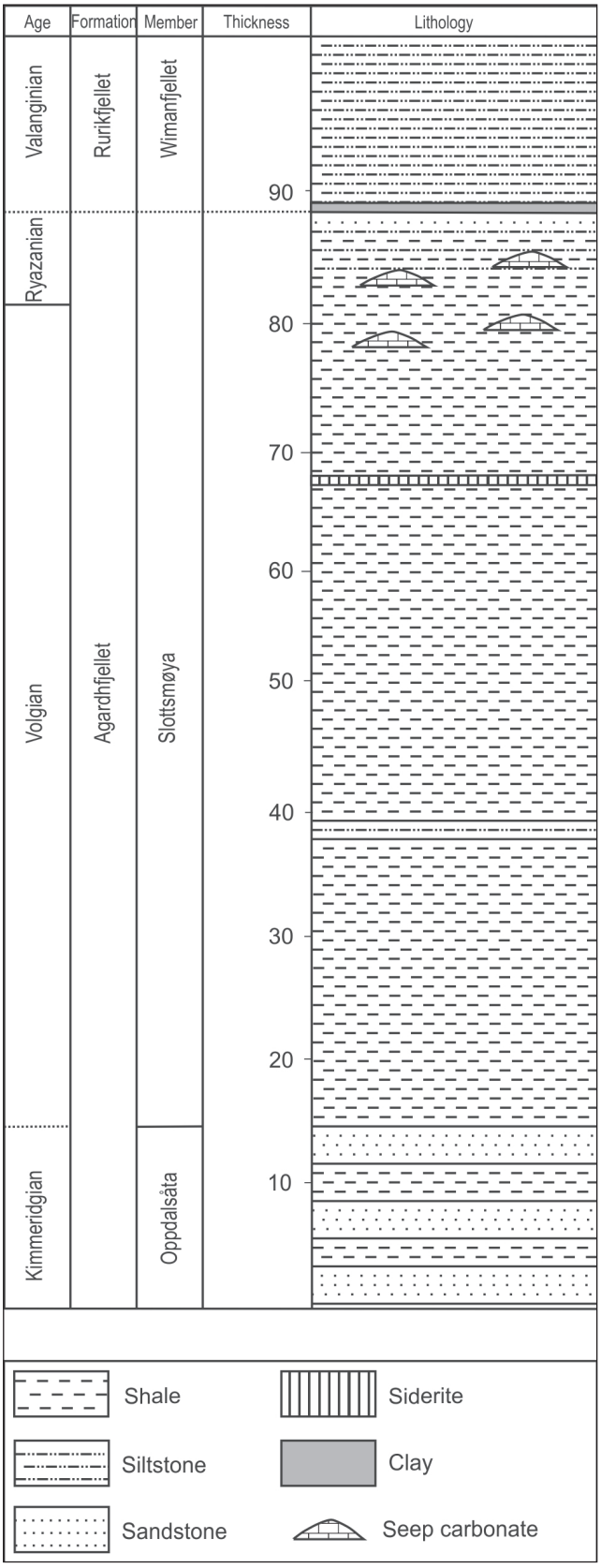


*Figure 2. Simplified lithostratigraphic log of the Slottsmøya Member in the southern Sassenfjorden area. Thicknesses given after Hammer et al. (2011).*

coast as distant as a few hundred kilometres to the north-east (Dypvik et al. 2002). The deposition of the uppermost Slottsmøya Member was affected by a markedly reduced sedimentation rate and probably by erosion due to tsunami waves, caused by the Mjønir impact a few hundred kilometres to the south in the Barents Sea (Dypvik et al. 2004, Wierzbowski et al. 2011).

According to the ammonite biostratigraphy, the Sassenfjorden hydrocarbon seep carbonates range from the basal Late Volgian to the latest Ryazanian (Fig. 3). According to Ogg et al. (2012), this should represent a time span of approximately nine m.y. If the Jurassic-Cretaceous boundary is positioned within the Upper Volgian Taimyrensis Zone, only seeps 3, 8 and 13 are Tithonian, whereas most of Sassenfjorden seep carbonates with known stratigraphy should be correlated with the Berriasian (Fig. 3; for details of Sassenfjorden seep carbonate stratigraphy, see Wierzbowski et al. 2011 and references therein).

## Materials and methods

In order to identify the earliest processes affecting the formation of the seep carbonates, we applied microfacies analysis to the Sassenfjorden seep carbonates. The accessibility and quality of the material allowed us to analyse nine out of 15 carbonate bodies. The analysis has been performed on uncovered thin sections (48 mm x 28 mm) prepared from unoriented and oriented samples. Thin sections were investigated under an optical microscope in plane-polarised and cross-polarised light for the identification of the carbonate minerals. The distinction between calcitic and non-calcitic mineralogy was possible after staining the thin sections in Alizarin-S solution (Friedman 1959). Non-carbonate opaque minerals were observed under reflected light optical microscopy to distinguish between sulphides and hydroxides. Definitions of different carbonate phases are based on Folk (1959). Carbonate microfacies terminology is after Dunham (1962) and Embry & Klovan (1971). The relative abundance of different types of grains was estimated using comparison charts for visual percentage estimation (Bacelle & Bosellini 1965 in Flügel 2004). Microscope photographs were made with a Leica DC 300 digital camera under the magnifications of 2.5, 5, 10, 20 and 40x. When necessary, the whole thin-section was scanned using a Nikon LS4000 slide scanner. In total, 344 thin sections were examined. Stable C isotope data have been obtained from 15 rock samples from two of the microfacies identified below; see Hammer et al. (2011) for analytical techniques.

## Results

Investigation of thin sections of the Upper Jurassic – Lower Cretaceous Sassenfjorden hydrocarbon seeps has

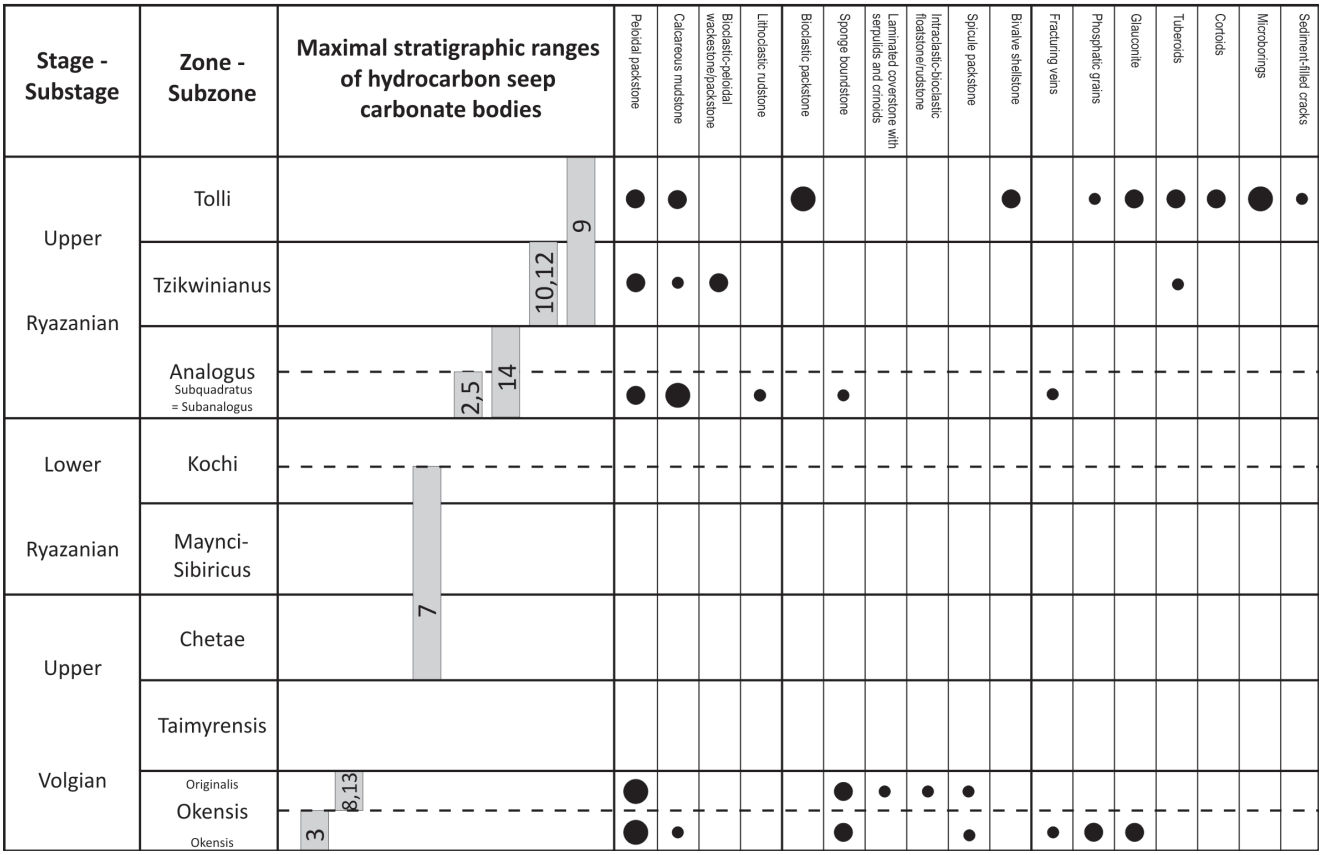


*Figure 3. Stratigraphy of the Sassenfjorden hydrocarbon seep carbonates and the stratigraphic distribution of described microfacies and sedimentary structures. Circle size indicates the relative abundance of the observed features; small = rare; medium = common; large = abundant. Modified from Wierzbowski et al. (2011).*

revealed the presence of ten depositional microfacies variably distributed among the nine investigated seep bodies. The bulk volume of the investigated carbonates is made up of only four dominant microfacies types, four are volumetrically important in some seeps only, whereas two other microfacies are only accessory features in a single seep. The microfacies are grouped into two sets, within which are subsets that are ordered volumetrically. Stable C isotope data for two of the volumetrically important microfacies are given in Table 1. We also identified two types of early diagenetic structures in the seeps, and three types of microborings in fossil shells.

## *Microfacies set I*

### Peloidal packstone

This microfacies type (Fig. 4A) has peloids reaching up to ≈ 1 mm in diameter variously dispersed in a recrystallised matrix. The $\delta^{13}C$ values of this microfacies range from -43.22 ‰ to -33.00 ‰ (Tab. 1). The primary porosity varies from around 20% to more than 40%. A nodular fabric is common, indicating several recurring stages of corrosion and grain cementation (Fig. 4A, B). Three types of grains are present in the peloidal packstone. The most common grains (around 90%) are brown peloids, composed of recrystallised micrite with a variable admixture of small allochem grains (Fig. 4B). Some of them are filled with euhedral dolomite (Hammer et al. 2011, fig. 4c). A few of the smaller peloids, not exceeding 500 μm in diameter, show signs of seven or nine longitudinal grooves on the outer surface (Fig. 4C). The second grain type is coated grains with opaque minerals in the core, surrounded by a carbonate envelope that usually consists of calcitic pseudomorphs after acicular

*Figure 4. Microfacies of the Volgian-Ryazanian Sassenfjorden seep carbonates. A) Peloidal packstone, grey arrow points to a small nodule. Seep 15, PMO 214.991. B) Detail of a bigger nodule with two stages of corrosion visible (white and grey arrows, respectively). Seep 5, PMO 214.938. C) Detail of a peloid with longitudinal grooves on the surface. Seep 10, PMO 214.976. D, E) Detail of a grain with a black core in transmitted and reflected light, respectively. White arrows point to peloids with a pyritic core; the grey arrow points to a peloid with an oxidised core surrounded by pseudomorphs after acicular gypsum. The asterisk on Fig. 4D indicates a sponge spicule with traces of an internal canal. Seep 3, PMO 214.968. F) Detail of rounded (left) and angular (right) phosphatic grains, surrounded by carbonate micritic cover. White arrow points to a glaucony grain enclosed within the phosphate. Grey arrow points to a small peloid enclosed within phosphate. Seep 3, PMO 214.975. G) Matrix of peloidal packstone. Grey arrow points to a fragment of an articulated hexact spicule network. White arrows point to glaucony grains. Seep 3, PMO 214.966. H) Detail of a sponge gemmule. Seep 13, PMO 171.024E.*

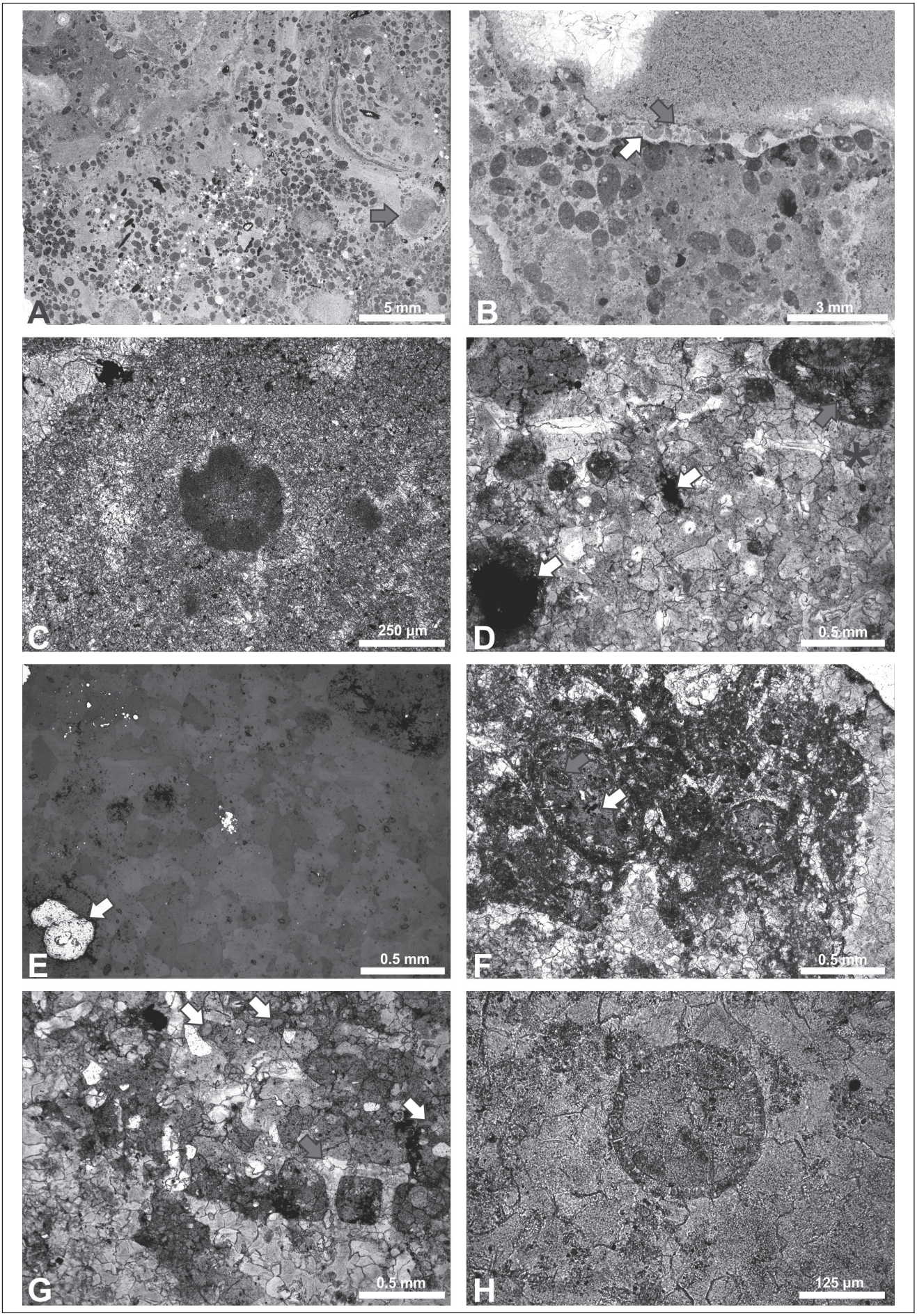
A
5 mm
B
3 mm
C
250 µm
D
0.5 mm
E
0.5 mm
F
0.5 mm
G
0.5 mm
H
125 µm

gypsum (Fig. 4D). Much less commonly, these coated grains are filled with framboidal pyrite aggregates (Fig. 4E). The third, and least common, type of grains in the peloidal packstone have variable amounts of phosphate in their cores. The phosphatic core may contain various amounts of dispersed detrital material. These grains are surrounded by carbonate envelopes which show weak traces of lamination (Fig. 4F). The recrystallised carbonate matrix hosting the grains in the peloidal packstone contains dispersed clastic material. Glaucony grains (Fig. 4F, G) and quartz silt are quite common, but never reach significant amounts. The most common are bioclasts consisting of well preserved phosphatic shells of lingulid brachiopods and sponge remains. Sponges are preserved either as calcite-replaced discrete spicules with remnants of the internal canal visible (Fig. 4D) or fragments of articulated hexacts (Fig. 4G). Another type of sponge remains is represented by spherical cysts made of a single chamber reaching up to 250 μm in diameter, surrounded by a row of short (≈ 10 μm) spicules perpendicular to the surface. We interpret these cysts as fossil sponge gemmules (Fig. 4H). The peloidal packstone microfacies hosts fossil tubes two to four mm in diameter (Fig. 5A), which are filled with later cements or with geopetal microspar (Hammer et al. 2011, fig. 5d). Some of these tubes are covered by isopachous carbonate cement, and they commonly show traces of wall delamination (Fig. 5A). In the vicinity of tubes the peloidal packstone is often corroded and encrusted by pyrite.

Table 1: $\delta^{13}C$ isotope composition of two main microfacies from seep locality 9

| Microfacies | $\delta^{13}C$ |
|---|---|
| Peloidal packstone | −32.00 |
| Peloidal packstone | −34.29 |
| Peloidal packstone | −34.39 |
| Peloidal packstone | −36.27 |
| Peloidal packstone | −37.80 |
| Peloidal packstone | −43.22 |
| Calcareous mudstone | −15.15 |
| Calcareous mudstone | −16.21 |
| Calcareous mudstone | −17.65 |
| Calcareous mudstone | −18.28 |
| Calcareous mudstone | −18.69 |
| Calcareous mudstone | −19.53 |
| Calcareous mudstone | −21.49 |
| Calcareous mudstone | −22.12 |
| Calcareous mudstone | −23.33 |

Calcareous mudstone

This microfacies type (Fig. 5B) was found in eight of the seeps investigated (Fig. 3). In seeps 2 and 5 it forms the bulk of the carbonate volume; however, most of the investigated carbonates are composed of lithologies other than micrites. The $\delta^{13}C$ isotope values range from – 23.33 ‰ to -15.15 ‰ (Table 1). The calcareous mudstone microfacies is formed mainly of grey to brown calcitic micrite (crystallites < 4 μm in diameter), but patches of coarser texture indicate local recrystallisation of micrite into microsparite. Small micritic nodules are commonly lined with a pyritic coating (Fig. 5B); framboidal pyrite is also generally dispersed in the calcareous mudstone. In places, the matrix is bioturbated, represented by irregular bands of disturbed sediment and diverging burrows up to 500 μm in diameter (Fig. 5B). In the bioturbated matrix, allochems are unevenly distributed and are represented by quartz sand, as well as dispersed glaucony grains, bioclasts, including calcareous and agglutinated foraminifera, fragments of shells and sporadic sponge spicules. In seep 2, the calcareous mudstone microfacies hosts rare fossil tubes (Fig. 5B).

Bioclastic-peloidal wackestone/packstone

This rare microfacies is found in a few samples from seeps 10 and 12. It is characterised by bioclasts and infrequent lithoclasts embedded in microsparitic matrix with peloids (Fig. 5C). Some of the bioclasts are embedded in brown, recrystallised micrite. The bioclasts are represented mainly by angular and unabraded bivalve and brachiopod shell fragments, and rare crinoid fragments. The bivalve shells can be recognised by blocky-calcite replacement in constrast to the brachiopod shells which show a primary foliated structure. Complete articulated bivalve and brachiopod shells are filled with peloidal carbonate or dolomite. Where present,

*Figure 5. Microfacies of the Volgian-Ryazanian Sassenfjorden seep carbonates. A) Detail of a tubeworm fossil from the peloidal packstone microfacies. Grey arrow points to tube wall delamination. Note botryoid growing on the external surface of the tube wall. Seep 9, PMO 171.025A. B) Calcareous mudstone. Grey arrow points to a worm tube fossil, white arrow points to a diverging burrow. Seep 2, PMO 215.008. C) Bioclastic-peloidal packstone. Note the articulated bivalve filled with dolomite and calcite spar. Seep 15, PMO 214.989. D) Lithoclastic rudstone. White arrow points to peloids between bigger lithoclasts. Seep 1, PMO 214.959. E) Bioclastic grainstone. Note imbrication and micritisation of some bioclasts. Seep 9, PMO 214.706. F) Cortoid with original lamellar structure of bivalve shell preserved intact. White arrow points to microboring parallel to the bioclast surface. Grey arrow points to thin microborings penetrating inside the bioclast. Seep 9, PMO 214.776. G) Heavily micritised and microbored bioclast. White arrow points to peloids originating from decomposition of micritised bioclasts. Seep 9, PMO 214.726. H) Detail of a tuberoid. Seep 9, PMO 214.772.*

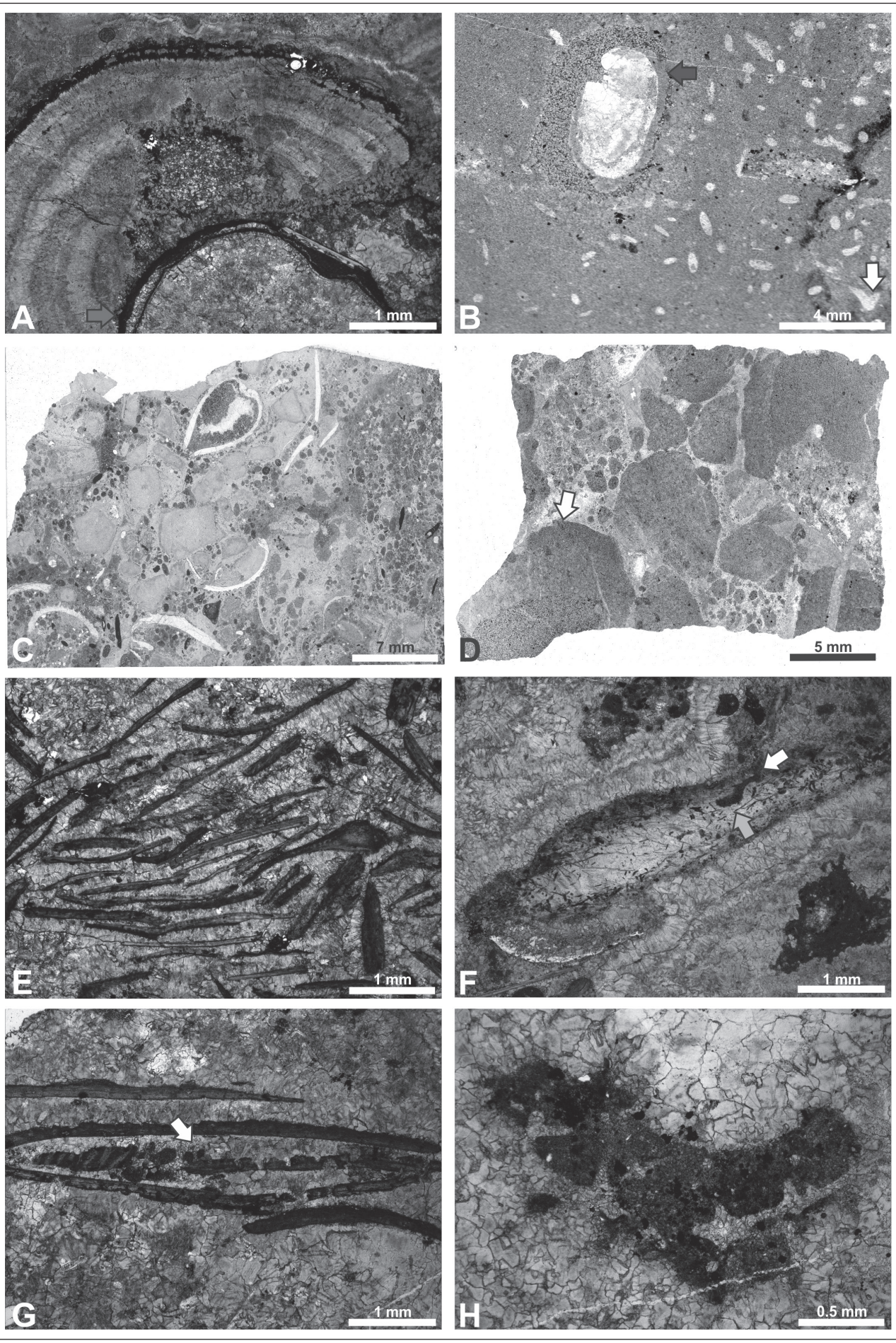
A
1 mm
B
4 mm
C
7 mm
D
5 mm
E
1 mm
F
1 mm
G
1 mm
H
0.5 mm

larger lithoclasts of micritic or peloidal carbonate show irregular corroded outlines and are covered with a thin pyrite lining. The percentage of clasts in the bioclastic-peloidal wackestone/packstone microfacies is variable, ranging from ≈ 20% to 60%. The matrix is composed of microspar containing dispersed peloids up to two mm long. The whole rock is sometimes transected by sediment-filled cracks.

Lithoclastic rudstone
This microfacies is common in seep carbonate 1 and consists of a peloidal matrix hosting subrounded to subangular lithoclasts (Fig. 5D). The lithoclasts of strongly recrystallised brown micrite in places have their centres filled with coarse-crystalline carbonate. No traces of corrosion or pyrite linings have been observed in the outer surfaces of the lithoclasts. Some lithoclasts are fractured, with cracks filled with sparitic cement. The total amount of lithoclasts in the rock volume can vary from 25 to 40 %. The matrix of the lithoclastic rudstone is formed of recrystallised peloids and small rounded lithoclasts reaching up to 30% of the rock volume. The remaining volume is occupied by sparite.

*Microfacies set II*

Bioclastic grainstone
This microfacies is present exclusively in seep 9, where it forms more than a third of the total volume of the carbonate body (Fig. 3). It comprises bioclasts, coated grains and lithoclasts with sparite filling the pore space (Fig. 5E). The total volume of all clasts varies from 20% up to 40%, depending on the degree of compaction. More than 90% of all bioclasts are flat, imbricated, shell fragments of bivalves and brachiopods, which form a cemented hash. Bivalve shells are dominant, and commonly have the original lamellar shell structure preserved (Fig. 5F). The shelly bioclasts measure from ≈ 200 μm to more than 15 mm in length and from less than 100 μm to about 2 mm in thickness. Due to intensive microerosion, larger bioclasts are often abraded and worn to cortoids, defined as grains surrounded by a penetrative, destructive, micritic cover (Fig. 5F). Heavily micritised bioclasts have fallen apart prior to diagenesis resulting in multiple, smaller, micritic grains (Fig. 5G). The 10% of non-bivalve and brachiopod bioclasts comprise serpulid tubes, both isolated and encrusting larger bioclasts, and calcareous benthic foraminifera, represented by species of *Lenticulina, Astacolus, Lingulina, Marginulina, Globulina* and *Epistomina* (for details see Hjálmarsdóttir et al., 2012). One unidentified specimen of an encrusting benthic foraminiferan has also been found.

The carbonate matrix of the bioclastic grainstone microfacies contains various amounts of glaucony and phosphatic grains. Glaucony can sometimes be present in significant amounts, giving the rock a characteristic green coloration. The amount of glaucony is positively correlated with the amount of quartz, which in extreme cases can comprise around 50% of the rock volume, giving it a calcareous sandstone appearance. Accessory, but very characteristic, clasts found in bioclastic grainstone are tuberoids (Fig. 5H), defined as rounded to subrounded micritic grains resulting from fragmentation of biocalcified sponges above the sediment/water interface. Tuberoids are the only sponge remains found in seep 9. They are accompanied by peloids reaching up to 500 μm in diameter, and by corroded intraclasts. The bioclastic grainstone microfacies is cemented by several generations of early and later cements.

Sponge boundstone
This microfacies was found in seeps 2, 3, 5, 8 and 13 (Fig. 3). It is characterised by sponge fossils within a peloidal matrix (Fig. 6A). The sponges are undeformed and relatively undamaged, with a detailed morphology visible in cross-section. The outer walls of the sponges are commonly marked by a thin lining of pyrite-rich micrite, which in places also lines the cloaca. The sponges are filled with microspar and botryoidal carbonate, and their soft tissues and skeletal substances are replaced by botryoidal spar (Fig. 6A). The sponge spicules are mainly hexacts and rare tetraxons, and they are invariably replaced by blocky calcite. The spicules are more abundant in the micrite-rich peripheries of the sponges, but somewhat less common in the botryoidal phase replacing most of the sponge skeletal and fleshy substances. In places, the sponges are uniformly replaced by a botryoidal carbonate without any visible body outline, leaving only a net of articulated calcite-replaced spicules (Fig. 6B).

Laminated coverstone with serpulids and crinoids
This microfacies consists of calcite-cemented material arranged in layers up to 1 cm thick (Fig. 6C). The upper and lower surfaces of successive layers are wavy and often show signs of truncation, corrosion and repeated carbonate precipitation, which can be marked by

*Figure 6. Microfacies and early diagenetic structures of the Volgian-Ryazanian Sassenfjorden seep carbonates. A) Sponge boundstone. Grey arrows point to pyrite lining the external and internal surfaces of a sponge. Seep 8, PMO 215.018. B) Detail of an articulated net of spicules within corroded calcite spar. Seep 8, PMO 215.017. C) Laminated coverstone with serpulids and crinoids. White arrow points to a pyritic lining on an intraclast. Grey arrow points to a serpulid tube. Seep 13, PMO 171.023B. D) Intraclastic/bioclastic floatstone. White arrow points to a fragment of a serpulid tube with no internal filling. The large horizontal crack is an artifact produced during sample preparation. Seep 8, PMO 215.016. E) Spicule packstone. White arrows point to corrosive outline. Seep 3, PMO 214.975. F) Bivalve shellstone. Note the geopetally arranged peloids partially filling the bivalve shells. Seep 9, PMO 214.715. G) Hydrofracturing veins. Note the spider-shape pattern in the upper-middle part of the picture (white arrow). Seep 3, PMO 214.869. H) Sediment-filled crack. White arrow points to a quartz grain. Seep 9, PMO 214.806.*

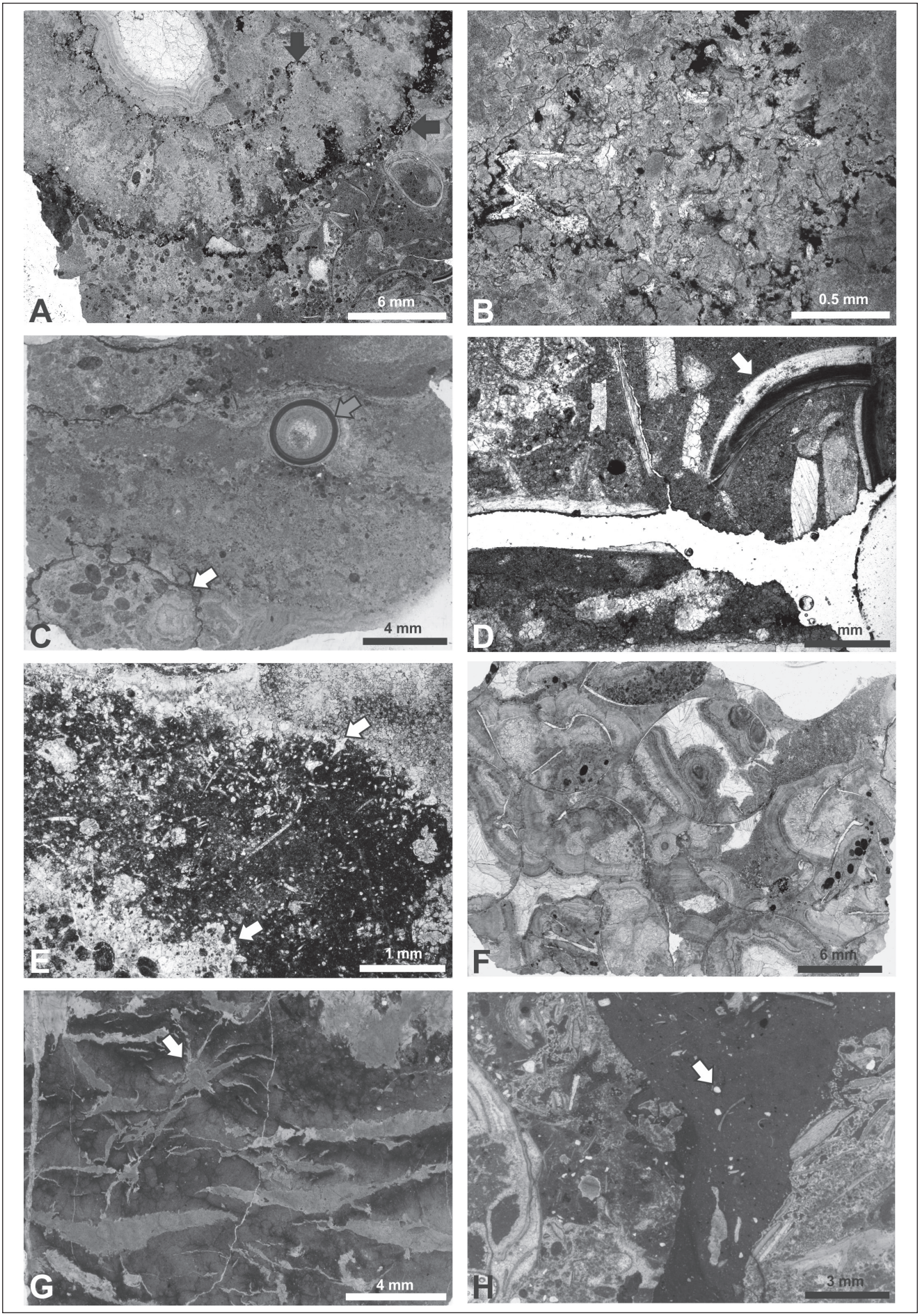
A
6 mm
B
0.5 mm
C
4 mm
D
mm
E
1 mm
F
6 mm
G
4 mm
H
3 mm

accumulations of small sparitic intraclasts, pyrite linings and by isopachous crusts of calcite-cemented silt. Small peloids, bioclasts and rare quartz grains are incorporated into each layer, together with sporadic, large, corroded and pyrite-covered intraclasts (Fig. 6C). The bioclasts comprise crinoid ossicles measuring up to 5 mm in diameter and serpulid worm tubes.

Intraclastic-bioclastic floatstone/rudstone
This microfacies has been found in seep 8. It is characterised by angular lithoclasts and fragmented bioclasts floating in a fine-grained carbonate matrix (Fig. 6D). The lithoclasts are those found in the layered coverstone microfacies, but rare fragments of peloidal facies also occur. The clasts are angular and lack pyrite linings; in the limited sample available they show no fitting. The bioclasts are sharp-edged fragments of serpulid tubes, with each fragment representing one quarter to a half of the original circumference of the tube. There are no signs of botryoidal cement filling the tubes. Unidentified shell fragments are also observed.

Spicule packstone
This is a very rare microfacies, preserved in seep 3 as isolated corroded intraclasts floating in the peloidal microfacies. It is characterised by an accumulation of disarticulated sponge spicules surrounded by calcareous micrite (Fig. 6E). The spicules are replaced by calcite and have various morphologies, dominated by monaxons, with some hexacts and tetraxons. Although disarticulated, the spicules are well preserved and no signs of breakage have been observed.

Bivalve shellstone
This microfacies is present in seep body 9 and consists of clusters of articulated or disarticulated (but relatively complete) bivalves (for species details see Hammer et al. 2011) surrounded by different generations of carbonate cements (Fig. 6F). The bivalve shells are replaced by blocky calcite; some are very thin and corroded, or sometimes completely absent, leaving only a mould. Complete shells and the shelter porosity between the disarticulated shells may be partially filled with peloids or recrystallised micrite, forming geopetal structures. The remaining space is occupied by later cements. The percentage of the shell material in the total volume of bivalve shellstone microfacies is below 10%.

## Early diagenetic structures

*Fracturing veins*

These structures have been found in thin sections from seep carbonate 3 and are visible on weathered surfaces of loose carbonate blocks from seep body 2 (Fig. 6G). The veins form enclaves of pointed, elongated (up to 3 cm or longer), thin (2-3 mm), parallel voids filled with botryoidal cements. They are present only in calcareous mudstone and are fabric-selective, since they terminate at microfacies boundaries. In the proximity of the veins the enclosing sediments are heavily cemented by botryoidal carbonate, which projects from the veins into the sediment. A characteristic feature of the veins is the presence of nets of crescent-shaped fractures projecting out from a central cavity and forming a spider-shaped pattern (Fig. 6G).

*Sediment-filled cracks*

Sediment-filled cracks are found in seep carbonates 9 and 10 (Fig. 3). They have been observed in the calcareous mudstone, peloidal packstone and bioclastic grainstone microfacies. They consist of wedge-shaped cracks a few centimetres in depth and not more than a few millimetres in width (Fig. 6H). The walls on the opposite sides of the cracks generally fit to each other, indicating no shear displacement after opening. The crack fillings are composed of calcareous mudstone with rare, floating, bio- and lithoclasts. Flow structures have been observed within the fillings. The bioclasts and lithoclasts derive from the walls, but have not been greatly displaced as they can be traced back to the point where they separated from the host rock. Elongated bioclasts are commonly oriented parallel to the walls.

## Microborings

Microborings are very common in bioclasts in the bioclastic grainstone microfacies from seep 9. Intensive decomposition of the larger bioclasts makes it difficult to estimate the total percentage of bioclasts affected by microborings, but this value is most likely very high, since the small and unbored bioclasts present in the microfacies derive mainly from the decomposition of intensively microbored larger bioclasts. The microborings can be grouped into three main types.

Type I microborings consist of tubular to club-shaped morphologies up to 300 μm long and around 50 to 80 μm wide, arranged perpendicularly to obliquely to the shell surfaces. They are usually solitary, but in places form clusters of three to eight. No branching has been observed. The internal walls of the microborings are flat or slightly curved (Fig. 7A), and are filled with dark calcareous micrite with varying amounts of disseminated pyrite.

Type II microborings have tubular morphologies and are concentrated slightly below and parallel to the shell surfaces (Fig. 7B). When the shell surfaces are corroded, the type II microborings lie directly below the surfaces and in cross-section are visible as shallow, bulbous depressions (Fig. 7B). Truncations are rare. Since the circular cross-section and diameter (up to 100 μm) are similar to type I microborings, we infer that they form one system. Single examples may be as thick as ≈ 300 μm in diameter. The filling consists of sparry calcite or dark micrite.

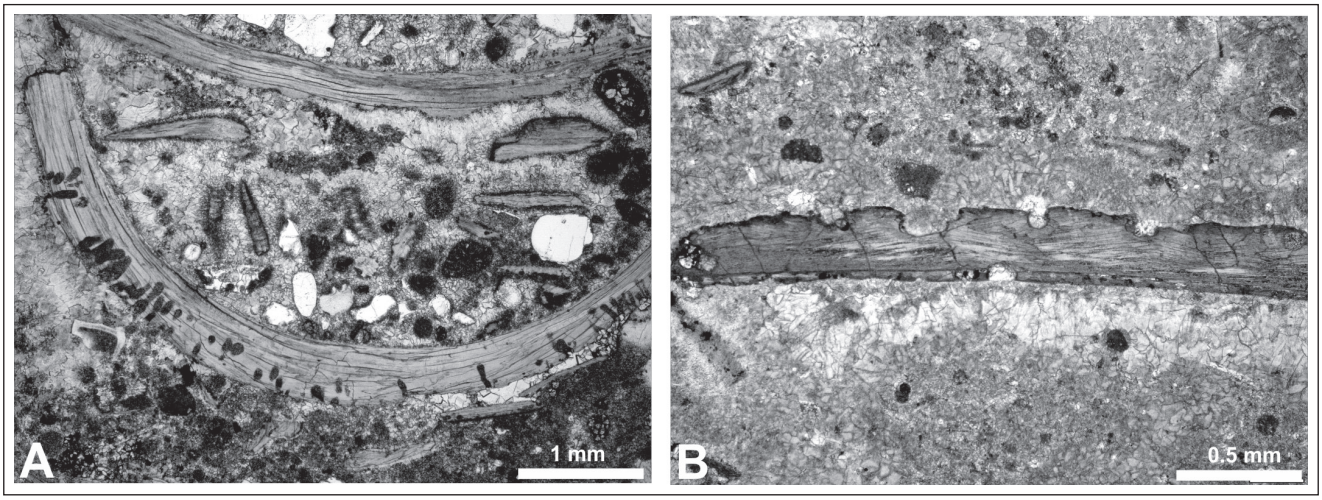


*Figure 7. Early diagenetic structures and microborings from the Volgian-Ryazanian Sassenfjorden seep carbonates. A) Tubular microborings formed in a brachiopod shell. Seep 9, PMO 214.744. B) Cross-sections of possible tubular microborings parallel to the shell surface. Seep 9, PMO 214.726.*

Type III microborings consist of relatively rare, thin (from 5 up to 30 μm), long microborings penetrating the whole thickness of the bioclast (Fig. 5F). They are dendritic and branch either at right angles or at acute angles, thus giving characteristic, antler-shaped patterns. Thin (5 to 20 μm) elongated galleries of microborings located directly below the surface of the bioclasts probably represent the same system, although the branching patterns of these is unknown.

## Interpretations

*Microfacies set I - early carbonate formation within the sediment*

The most common type of microfacies in the studied seep carbonates (Fig. 3) is peloidal packstone (Fig. 4A). The rounded to ovoid shape of the peloids, together with their sharp boundaries and considerable quantities of incorporated detrital material, are indicative of a faecal origin (Flügel 2004). Dolomite crystals filling the peloids (Hammer et al. 2011, fig. 4c) were most likely formed during a later diagenetic event and were thus not initially present within the peloids (Beauchamp & Savard 1992, Gaillard et al. 1992, Kelly et al. 1995). Definitive crustacean faecal peloids *Favreina* and *Palaxius* have been identified in Oxfordian hydrocarbon seep deposits in Beauvoisin in southern France (Senowbari-Daryan et al. 2007) and in Eocene methane-seep limestone from the Humtulips Formation in Washington (Peckmann et al. 2007). Although the Sassenfjorden seep peloids are within the size range of these examples, it would be unwise to attribute the bulk of the Sassenfjorden peloids to crustacean faecal pellets since they lack the conspicuous and taxonomically important patterns of internal longitudinal canals (Brönnimann 1972). Moreover, in recent hydrocarbon seeps crustaceans are common, but they never occur in numbers high enough to explain such a accumulation of faeces as in the Sassenfjorden seeps (e.g.,. Barry et al. 1996, Olu-Le Roy et al. 2004, cf. Sibuet & Olu 1998, Levin 2005).

The Sassenfjorden seep peloids might instead have been produced by other groups of deposit-feeding organisms, including polychaetes (cf. Fauchald & Jumars 1979), protobranch bivalves, irregular echinoids and holothurians. Deposit-feeding protobranch bivalves produce rods of expelled faeces (e.g., Cox 1960, Zardus 2002), which are susceptible to fragmentation and can give peloids with conspicuous longitudinal grooves on the surface (Cox 1960, fig. 2). Some of the Sassenfjorden seep peloids are unstructured internally with an odd number of longitudinal grooves (Fig. 4C), and protobranch bivalves are common in the seep carbonates (Hammer et al. 2011), which could indicate a causative link. Irregular

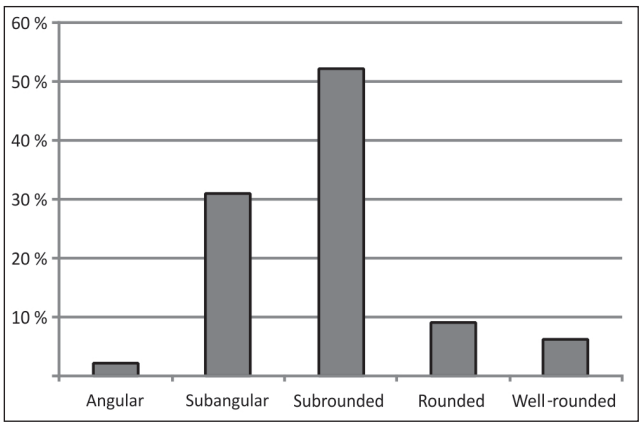


*Figure 8. Relative percentage of particular groups of bioclast shapes in bioclastic grainstone. N=100.*

echinoids are deposit feeders known to produce faecal pellets of undigested sediment (e.g., Kier 1972, pl. 2, fig. 2) which are within the range of sizes encountered in Sassenfjorden seep peloids. Some irregular echinoids possess symbionts and are encountered in the vicinity of recent and fossil cold seeps (Temara et al. 1993, Van Dover et al. 2003, Olu-Le Roy et al. 2004, Gaillard et al. 2011), where they are believed to benefit from the local chemosynthetically produced organic matter. No examples are known from the seep carbonates, nor from the earlier part of the Slottsmøya Member (Rousseau & Nakrem 2012). However, if they were also present in the seeps they may have contributed to the observed sediment reworking within them. Among other organisms, holothurians are worth mentioning. They are burrowers producing faeces several centimetres in length, which usually decompose in hours after formation (Conde et al. 1991). However, carbonate authigenesis inside burrows of holothurians (e.g., Haas et al. 2010) has been postulated as one of the possible mechanisms of carbonate authigenesis in recent cold seep carbonates, but application of this mechanism to the Sassenfjorden seeps is problematic since no obvious burrows have been found within the seep carbonates.

An allochthonous origin for the peloidal material is unlikely since the nearest shallow-water environments were distant and devoid of carbonates (Dypvik et al. 2002) and the Slottsmøya Member is characterised by a low-energy, deep to middle shelf setting with no turbidite deposits (Dypvik et al. 1991b). An autochthonous origin by winnowing of fines by currents is also unlikely since the depositional environment was too deep for wave action to have had any influence on the sediment (see Pratt et al. 2012 for comparison). A more plausible explanation for the accumulation of faecal pellets in the Sassenfjorden seep carbonates is that they were locally produced by various deposit feeders and later condensed by removal of fine material due to fluid flow at the seep site.

One of the grain types in peloidal packstone mixed with faecal peloids comprises irregular coated grains with a pyritic core and carbonate envelope. They are most likely associated with a localised process of anaerobic oxidation of methane resulting in the formation of pyrite aggregates covered with carbonate. Similar coated grains have been recorded in the Campanian Yasukawa seep in Hokkaido (Jenkins et al. 2008) and from Eocene grapestone concretions from near Varna, Bulgaria (De Boever et al. 2011). However, these grains are not directly comparable with the coated grains from the Sassenfjorden seep carbonates. The Varna examples are single-coated grapestones exceeding 15 cm in diameter and are believed to originate through multistage formation of carbonate at the surface of the seep (nuclei) and in shallow burial (cortex). The Varna grapestone nuclei do not exceed 2 mm in diameter and they, rather than whole concretions, are more comparable to the Sassenfjorden grains. The Sassenfjorden seep coated grains are more similar in size to the cores of Yasukawa grains, which are interpreted to have originated at around the sediment-water interface. However, the cores of the Yasukawa coated grains are composed of fractured siliciclastic sediment (Jenkins et al. 2008, fig. 3, 4) in contrast to the pyritic nuclei (Fig. 4D, E) of the Sassenfjorden seep grains. The Sassenfjorden coated grains were then likely to have formed in less vigorous fluid flow than their Yasukawa equivalents, and their formation did not involve fracturing of surficial sediments. The pyrite aggregates indicate that the coated grains probably formed within the sediment at shallow depths where sulphate reduction coupled with anaerobic oxidation of methane was possible. Asymmetric grain shapes resulted from grains pressing against one another as they grew within the sediment. Oxic conditions during later stages of grain growth oxidised the pyrite in the core to opaque minerals such as iron oxyhydroxides and gypsum (Fig. 4D).

Another grain type found within the peloidal packstone microfacies is that of grains with phosphatic cores (Fig. 4F). The relative timing of the formation of these grains remains difficult to estimate. They may have formed before the seepage commenced and were coated during carbonate authigenesis, or they may have formed close to the surface within the existing hydrocarbon seep carbonate. The presence of carbonate particles within the phosphate (Fig. 4F) supports the latter interpretation.

The bioclastic/peloidal wackstone/packstone microfacies (Fig. 5C) found in seeps 10 and 12 seems to be a variety of the peloidal facies with a greater proportion of bioclasts. The greater volume of bioclasts may indicate a shallower depth of formation or with an ecological succession due to a longer duration of methane flux (Sahling et al. 2002, Jenkins et al. 2007). Fragments of epifauna (e.g., crinoid ossicles) inferred to benefit from hardgrounds (shells and exhumed seep carbonate), encapsulated within this carbonate microfacies, indicate that the carbonate authigenesis took place close to the sediment-water interface. Rapid cementation is shown by sediment-filled cracks (Fig. 6H). However, the general mode of authigenesis (formation of carbonate within pelletised sediment) remains the same.

The grains within the peloidal packstone microfacies come from pelletisation of mud by deposit feeders and from an authigenic precipitation of non-carbonate minerals. All of them were formed within the sediment in the shallow subsurface. The accumulation of these grains within the sediment increased the porosity and permeability with respect to surrounding muds. The relatively impermeable muds diverted large amounts of fluids into the permeable pelletised sediments. This favoured fluid flow and resulted in more abundant methane-derived carbonate cementation within pelletised sediment, giving a peloidal appearance to the bulk of the carbonate and only a minor contribution of micritic facies. In contrast, in more permeable sediments like silts and sands a more diffusive flow was

favoured, resulting in the formation of calcareous mudstone (Beauchamp & Savard 1992, Campbell 1992, 2006, Greinert et al. 2001, Campbell et al. 2002). With progressive substrate cementation, worm tube fossils, showing some similarities with vestimentiferan tubes (i.e., delaminated wall, Peckmann et al. 2005, Himmler et al. 2008, Haas et al. 2009; Figs. 5A, 5B), could have acted as fluid conduits. Since peloidal packstone together with calcareous mudstone are among the most abundant microfacies in the Sassenfjorden seeps and they are found in all of the seeps investigated, we infer that they constitute the core facies of the Sassenfjorden seep carbonates. Since mudstones commonly contain well preserved burrows filled with carbonate cement, the formation of the seep carbonate must have take place at depths of dozens of centimetres below the sediment-water interface at most, which is usually the situation in recent cold seeps (e.g., Hovland et al. 1987, Naehr et al. 2000, Tsunogai et al. 2002, cf. Levin 2005, Campbell 2006) where the process of anaerobic oxidation is at its most intensive (Boetius et al. 2000).

The fluid flow pattern within pelletised sediment was probably responsible for the difference in isotopic composition between the peloidal packstone and the calcareous mudstone. In seep 9, the peloidal packstone microfacies has a more depleted $\delta^{13}C$ isotope composition than the calcareous mudstone microfacies (Hammer et al. 2011). This can be explained by more intensive fluid flow within permeable pelletised sediment and incorporation of light organic carbon from the initial pool that was constantly resupplied in depleted carbon by fluid flow (Table 1). In less permeable mudstone the carbon pool of fluid was restricted due to weak flow, which resulted in a smaller absolute pool of light carbon available for crystallisation, and heavier carbon isotopes were gradually added from pore waters. In consequence, this led to a less depleted signature in the authigenic calcareous mudstone microfacies. The restricted fluid flow within the calcareous mudstone is further testified by the development of fracturing veins, which we suggest were the result of hydrofracturing episodes. Lower initial permeability resulted in overpressuring, which was occasionally released forming crescent-shaped fractures filled with botryoidal calcite. These rapid pressure-release episodes caused desintegration of calcareous mudstones and formation of lithoclastic rudstones with injection of peloids into the openings (Fig. 5D). It is also likely that the heavier isotopic values of the sampled mudstones compared with the peloidal packstone resulted from multistage formation of mudstones and incorporation of heavier carbon isotopes during later diagenesis (Peckmann & Thiel 2004). However, bioturbation and early brecciation indicate that at least some micrites formed at early stages.

*Microfacies set II - early carbonate formation near the sediment/water interface*

The laminated coverstone microfacies (Fig. 6C) from seep 13 can be interpreted as fossil laminated crust formed close to the sediment/water interface in relatively permeable sediment (e.g., Olu-Le Roy et al. 2004, fig. 2d; Feng & Roberts 2010). In the Svalbard seep carbonates, this is indirectly indicated by the presence of serpulid worm tubes enclosed within the coverstone carbonate. The intraclastic-bioclastic floatstone/rudstone is probably an effect of disintegration and brecciation of these facies close to the sediment-water interface. A possible factor responsible for such brecciation was episodes of rapid release of overpressurised fluids, as described in the previous section, or the collapse of the carbonate overhanging cavities (e.g., Judd & Hovland 2007, fig. 2.37).

The Late Volgian (localities 3, 8 and 13) and the earliest Late Ryazanian seeps (localities 2 and 5) contain relatively large numbers of well preserved sponges. Siliceous hexacts with internal channel indicate siliceous sponges, but rare tetraxons diverging at a 120° angle show that demosponges were also present (de Laubenfels 1955). Recent glass sponges are most common in moderately deep marine settings at depths between 300 and 600 metres (Leys et al. 2007), but in the Late Jurassic Peritethyan area they formed extensive belts of bioconstructions in shallow water (Flügel & Steiger 1981, Leinfelder et al. 1993, Trammer, 1989, Krautter 1997, Pisera 1997, Olóriz et al. 2003). However, their presence on Svalbard does not coincide with the Oxfordian acme of glass sponges and is probably ecologically controlled, since they also occur in Oligocene seep deposits (Rigby & Goedert 1996).

Siliceous sponges and demosponges are susceptible to early biocalcification (e.g., Neuweiler et al. 2007) because of the presence of protein components together with silica in their skeletons (de Laubenfels 1955). The degrading organic macromolecules are known to bind $Ca^{2+}$ and $Mg^{2+}$ ions on their surface, thus enabling nucleation of carbonate minerals in environments with increased alkalinity (Reitner 1993). This model of biocalcification can be applied with some restrictions to the Sassenfjorden seep material. In hydrocarbon seeps, a rise of alkalinity and formation of carbonate usually take place within the sediment (Greinert et al. 2002, Bayon et al. 2009) and bottom waters are only rarely affected (e.g., Reitner et al. 2005). The complete preservation of sponges in the Sassenfjorden seeps indicates that they were calcified rapidly where high alkalinity occurred and sponge tissues were protected from collapse after subsequent decay (Warnke 1995, Hammes 1995). The limited preservational potential of the sponges indicates that immediately prior to biocalcification they must have been populating the sea floor and they were calcified *in vivo* or very early *post mortem*. They probably colonised local carbonate hardgrounds exposed on the sea bottom, and were perhaps filter feeding on the free-living microbes, as has been recently suggested for geodiid demosponge assemblages from the Thuwal seeps in the northern Red Sea (Batang et al. 2012) or from the Queen Charlotte Sound off Canada (Vaughn

Barrie et al. 2011). Episodic deposition of thin blankets of sediment on top of the carbonate hardgrounds populated by sponges provided an additional volume of sediment for a rise in alkalinity and in consequence allowed sponge biocalcification. Uncovered sponges were not subjected to biocalcification and decomposed into accumulations of loose spicules, which were calcified in exceptional cases. The biocalcification within the sediment may have been coupled with sulphate reduction (i.e., Reitner & Schummann-Kindel 1997), giving a pyrite lining on the inner and outer surface of the sponge (Fig. 6A). Some of the calcified sponges may also have acted as fluid conduits.

We interpret the sponge boundstone microfacies as one of the surficial facies of the Late Volgian and earliest Late Ryazanian Sassenfjorden seeps (localities 3, 8, 13 and 2, 5, respectively). Another surficial microfacies found exclusively in seep 9 is bioclastic grainstone, composed predominantly of worn shell fragments (Figs. 6E, F, G). Microborings and serpulid tubes encrusting some of the bioclasts confirm that this sediment originated at the sediment/water interface. The bioclasts are mainly autochtonous and there is no evidence for long-distance grain transport (Fig. 8). The local imbrication of shells and absence of fine-grained material indicates some bottom current activity during formation, although winnowing due to high flux from the subsurface is another possible explanation for these observations. The smaller bioclasts originated from the decomposition of bivalve shells, found in large clusters in the same seep (Hammer et al. 2011). An autochthonous origin of most of the bioclasts in the bioclastic grainstone microfacies is also supported by the presence of brachiopods, which so far have not been identified outside seeps in the transitional Jurassic-Cretaceous sediments on Svalbard (Birkenmajer et al. 1982). Disarticulation of the shells resulted from a variable degree of micritisation (Bathurst 1966), and pervasive micritisation led to the decomposition and fragmentation of bioclasts into small detrital peloids (Fig. 6G). A similar process of clast micritisation and decomposition has been recognised in recent (Reid et al. 1992) and fossil (Samankassou et al. 2005) marine sediments. Peloids formed in this way are not synonymous with, and should not be confused with faecal peloids from peloidal packstone (see Flügel 2004, p. 110, for discussion of peloid terminology).

In bioclastic grainstone micritisation of the clast peripheries is associated with the occurrence of cortoids (Fig. 5F). These grains are bioclasts coated with either constructive (Kobluk & Risk 1977) or destructive, Mg-calcite, micritic cover (Bathurst 1966, Reid & Macintyre 2000). In shallow-water sediments the destructive cover is usually attributed to the activity of phototrophic microendoliths (Peryt 1983). This link seems rather unlikely in the Sassenfjorden seeps, which were located at outer to middle shelf depths, almost certainly below the photic zone (Dypvik et al. 1991b). It is likely that in the seep environment, cortoid development could be partially enhanced by intense activity of chemoautotrophic and heterotrophic microorganisms, forming films and mats on bioclastic substrates (e.g. Barbieri & Cavalazzi 2005). However, micritic covers developed preferentially around aragonite bivalve shell fragments and not on more resistant brachiopod and serpulid calcitic skeletal fragments (Fig. 7B). This indicates that micritisation was localised to less resistant aragonite and suggests that an inorganic process due to partial dissolution and recrystallisation was the causative mechanism (Winland 1968, Alexandersson 1972, Flügel 2004). This inorganic process usually affects aragonite or Mg-calcite, which lose Mg to the surrounding undersaturated fluids and turn into more stable low-Mg calcite with a lower concentration of Mg (Neugebauer & Ruhrmann 1978, Flügel 2004). A very early diagenetic origin of the calcite envelope is indicated by the preservation of the original lamellar structure of the bivalve bioclasts (Fig. 5F); the more resistant calcite prevented the dissolution of the original aragonitic structure during subsequent diagenetic stages (Winland 1968).

The Late Ryazanian seep 10 and especially the latest Ryazanian seep 9 contain remains of fossil glass sponges in the form of tuberoids (Fig. 5H). Tuberoid formation is a result of patchy biocementation of a decaying sponge body and takes place above the sediment column or in the shallow subsurface in yet uncemented sediment. After subsequent decomposition of sponges, tuberoids are spread around and mixed with other grains (Warnke 1995). In seeps 9 and 10 the presence of tuberoids, and micritised and microbored shells indicate prolonged residence on the sea floor. We interpret the change of mode of preservation of sponges within the Sassenfjorden seep carbonates from complete sponges (Late Volgian to earliest Late Ryazanian, Fig. 6A) to tuberoids (Middle to Late Ryazanian, Fig. 5H) as evidence for prolonged exposure on the sea bottom and increased time averaging within surficial sediments of seep 9 as compared with older seeps. In the Late Volgian to the earliest Late Ryazanian, the Sassenfjorden sponges were covered with mud which favoured their complete preservation. However, in the Late and especially latest Ryazanian bottom conditions prevented their preservation. Among the possible causes, omission by bottom currents removing the fines seems to be likely, especially in connection with the occurrence of glaucony and imbrication of bioclasts. The relative longevity of this seep could have enabled the mixing of tuberoids with large amounts of autochthonous, coarse-grained, shelly material even in a relatively low-energy setting.

Bioclasts and tuberoids in rock-forming amounts occur exclusively in seep 9. This may be a result of several coupled circumstances. Seep 9 is the only seep where clusters of bivalves developed (Hammer et al. 2011), providing an abundant supply of coarse-grained material. This is also the only seep spanning more than one ammonite

biochron (Wierzbowski et al. 2011), which may have influenced the amount of shell material available for condensation and, in consequence, enabled the formation of a lag of coarse-grained bioclastic grainstone. Moreover, seep 9 is markedly larger than the other seep carbonates, which influenced the volume of available shell material. It is possible that these factors acted as positive feedbacks and the accumulation of bioclasts enabled more substrate for colonisation by shelly organisms, again increasing the volume of accumulating bioclasts.

A phenomenon known from some recent pockmarks from shallow-water settings is concentration of coarse-grained material in the depression (e.g., Hammer & Webb 2010). The exact cause of this phenomenon remains unknown. It may, however, be linked with increased current activity inside pockmarks due to current deflection (Hammer et al. 2009). Similar processes have been observed in some recent examples (e.g., Bøe et al. 1998), where the increased current activity is likely to result in a relative enrichment of the coarser grains. The processes observed within seep 9, such as accumulation of autochtonous material, prolonged exposure on the sea bottom and removal of fine material by currents are in general agreement with processes observed in recent pockmarks. However, as stated above, the intense frost-wedging and permafrost-related slumping means that the original shape of the carbonate body and its relationship to the surrounding sediments is poorly constrained.

*Palaeobathymetry*

The bioclasts that accumulated in seep 9 contain various microborings, which can be used as a tool for estimating palaeowater depth (cf. Glaub 1994, Glaub & Bundschuh 1997). A similarity between recent and fossil forms allows the use of actualistic studies for palaeobathymetrical analysis. In the Sassenfjorden seeps, relatively rare, perpendicular, club-shaped microborings (Fig. 7A) are within the range of shapes and sizes represented by macrotubular forms sensu Glaub 1994 (see also Vogel & Brett 2009, fig. 35). Galleries parallel with the shell surface with the same range of diameters as macrotubular forms may be connected in a single system with perpendicular microborings. Macrotubular forms are smaller than most of the borings made by polychaetes (see Pemberton et al. 1988 for comparison) and are usually compared with fragments of systems made by phoronids (Voigt 1975, Glaub 1994). The facies-crossing character of these microborings attributed here to types I and II makes them less useful for palaeobathymetric reconstructions (Glaub 1994). It should be noted that the direct assignment of producer to specific microborings is connected with speculative simplifications (see discussion in Pickerill & Harland 1984), and forms similar in cross-section to the forms described herein can also be compared with undescribed microborings of presumed bryozoan origin (e.g., Vogel & Marincovich 2004, fig. 4.5) as well as with *Rogerella* isp. created by acrothoracican cirripedia (Senowbari-Daryan et al. 1993) or *Podichnus* isp. by the pedicle of articulated brachiopods (Bromley & Surlyk 1973). Whichever solution is chosen for the material in question, the microboring morphological types I and II were non-phototrophic and likely had wide bathymetrical distributions.

Type III microborings, composed of thin (up to 20 μm) galleries entangling around the bioclasts and in places penetrating inside, are also taxonomically problematic. Galleries parallel with the substrate are similar in size to fossils from the ichnogenus *Orthogonum*, which is sometimes attributed to fungi (Radtke 1991, Glaub 1994). However, it should be kept in mind that thin galleries entangling the bioclast can also be ascribed to other ichnogenera, like *Reticulina* or *Eurygonum*, and attributing the Svalbard material to any of these is not possible at the present time. Penetration of fungal hyphae inside the bioclasts is perfectly possible, but we have failed to find any bulbous chambers for sporangia to prove the fungal affinities of the microborers. Furthermore, the thin branches penetrating inside the bioclasts (Fig. 5F) and diverging at acute to right angles do not show a reticulate pattern and do not rejoin after diverging once, so a sponge affiliation is also possible (Pickerill & Harland 1984). As well as for microtubular forms, a non-phototrophic mode of nutrition can also be postulated here and such forms have been suggested to occupy all depths, though with greater accumulation in the deeper bathymetrical zones (Glaub 1994). This is in agreement with the outer to middle shelf interpretation of Dypvik et al. (1991b).

Indirect evidence for proximity to the photic zone is given by well preserved specimens of *Epistomina* sp., an aragonitic foraminiferal genus which is considered to be a grazing herbivore and accompany seaweeds (Reolid et al. 2008). It is also a sensitive indication of phytodetritus input (Reolid 2012, pers. comm.). Grazing on non-phototrophic microorganisms is, however, also a possible explanation for the presence of *Epistomina* sp. The specimens are well preserved and do not show any signs of transport (Hjálmarsdóttir et al., 2012, fig. 5k), They may come from pseudoplanktonic falls, as testified by abundant wood remains, scattered in the Sassenfjorden seep carbonates (Hammer et al. 2011) and in the entire Slottsmøya Member.

*Stratigraphic evolution*

The stratigraphic distribution of the Sassenfjorden seeps shows that the highest percentage of peloidal facies occurs especially in the Volgian seep carbonates (seep bodies 3, 8 and 13). The earliest Late Ryazanian seeps (seep bodies 1, 2 and 5) have features shared with the Late Volgian seeps (sponge microfacies) and the latest Ryazanian seep 9 (calcareous mudstones). In contrast to the Late Volgian, the latest Ryazanian seep is composed predominantly of calcareous mudstones (Fig. 3). A

similar distribution pattern is observed for the sponges, which are common in the Late Volgian seep carbonates and occur only sporadically within the earliest Late Ryazanian carbonates, being replaced by bioclastic grainstones with tuberoids in the latest Ryazanian. We infer that this trend observed in the stratigraphic distribution of microfacies is connected with a change in properties of the background sediments (Dypvik et al. 1991b, fig. 13). The Late Volgian seeps developed in relatively impermeable muds, where flow was restricted to narrow zones of pelletised sediments. This influenced the duration of flow and resulted in a self-sealing of seeps by the localised formation of carbonates (Hovland 2002), resulting in short-lasting seeps (Wierzbowski et al. 2011). The earliest Late Ryazanian seeps have some transitional features. The latest Ryazanian seep developed in more permeable silts and sands, which dispersed fluid flow and allowed long-lasting seepage.

All seeps investigated are developed in a condensed interval six metres in thickness (Fig. 2). Based on the profile presented by Dypvik et al. (1991b, fig. 13) and on discussion of the sedimentology of the overlying sediments (Dypvik et al. 1992), Wierzbowski et al. (2011, p. 274) connected the stratigraphic condensation of the seep interval with a general shallowing that took place during the whole seep interval, starting at least in the Late Volgian. The present study confirms the condensed nature of the interval investigated, with a possible change of sediment character in the uppermost part of the Slottsmøya Member just before the latest Ryazanian.

## Conclusions

1. The Sassenfjorden seeps represent the effects of seepage during a period of c.a. 9 m.y. in a low sedimentation rate setting.
2. Early carbonate formed within the sediment makes up the bulk of the authigenic carbonate. Carbonate formed around the sediment/water interface is volumetrically far less important.
3. Early carbonate formed within the sediment has relatively low diversity, comprising peloidal packstones and calcareous mudstones. Peloidal packstone is a result of faecal pellet accumulation by sediment removal by fluid flow and early carbonate authigenesis within permeable pelletised sediment. Calcareous mudstone is carbonate formed in impermeable muds in the immediate surroundings. Carbonate formed around the sediment-water interface comprises diverse carbonate microfacies, representing different microenvironments on the top of the seep carbonates. They are represented by carbonate slabs colonised by serpulids, sponges that inhabited the surface of the carbonate, and accumulation of disintegrated and worn shell fragments.
4. The microboring assemblage from the latest Ryazanian seep 9 consists mainly of heterotroph and chemoautotroph trace fossils. No obvious photoautotroph traces have been identified. Palaeowater depth in the latest Ryazanian thus exceeded that of the photic zone. The proximity of the photic zone, however, is indirectly indicated by the presence of algal-grazing foraminifera.
5. The Late Volgian to Late Ryazanian seeps developed in relatively impermeable muds. They were short-lasting due to obscured fluid flow and self-sealing of conduits by precipitating carbonate. Sediment changed to more permeable silts and sands before the latest Ryazanian. The latest Ryazanian seep developed in permeable silts and sands, which facilitated a more undisturbed fluid flow. The longevity influenced the size of this seep carbonate and resulted in the accumulation of large volumes of coarse-grained material.

*Acknowledgments*. - Fieldwork at Svalbard (2007–2011) was financed by the Norwegian Research Council, Norwegian Petroleum Directorate, Spitsbergen Travel, ExxonMobil, Fugro, Statoil, OMV, Powercontrols and Hydro, and by grants nos. EC0425-09 and EC0435-09 from the National Geographic Society. The authors are also grateful to all the volunteers and students who have contributed weeks of fieldwork for free on the project. Special thanks go to Nils-Martin Hanken for discussing some aspects of carbonate sedimentology and to journal referees Martin Hovland and Matías Reolid for their comments which improved this paper significantly.

## References

Alexandersson, E.T. 1972: Micritization of carbonate particles: process of precipitation and dissolution in modern shallow-water sediments. *Bulletin of the Geological Institute of the University of Uppsala, Natural Sciences 3*, 201-236.

Bacelle, L. & Bosellini, A. 1965: Diagrammi per la stima visiva della composizione percentuale nelle rocce sedimentarie. *Annali della Universitá di Ferrara, Sezione IX, Science Geologiche e Paleontologiche 1*, 59-62.

Barbieri, R. & Cavalazzi, B. 2005: Microbial fabrics from Neogene cold seep carbonates, Northern Apennine, Italy. *Palaeogeography, Palaeoclimatology, Palaeoecology 227*, 143-155.

Barry, J.P., Greene, H.G., Orange, D.L., Baxter, C.H., Robinson, B.H., Kochevar, R.E., Nybakken, J.W., Reed, D.L. & McHugh, C.M. 1996: Biologic and geologic characteristics of cold seeps in Monterey Bay, California. *Deep-Sea Research I 43*, 1739-1762.

Batang, Z.B., Papathanassiou, E., Al.Suwailem, A., Smith, C., Salomidi, M., Petihakis, G., Alikunhi, N.M., Smith, L, Mallon, F., Yapici, T. & Fayad, N. 2012: First discovery of a cold seep on the continental margin of the central Red Sea. J*ournal of Marine Systems 94*, 247-253.

Bathurst, R.G.C. 1966: Boring algae, micritic envelopes and lithification of molluscan biosparites. *Geological Journal 5*, 15-32.

Bayon, G., Henderson, G.M. & Bohn, M. 2009. U-Th stratigraphy of a cold seep carbonate crust. *Chemical Geology 260*, 47-56.

Beauchamp, B. & Savard, M. 1992: Cretaceous chemosynthetic carbonate mounds in the Canadian Arctic. *Palaios 7*, 434-450.

Birkenmajer, K., Pugaczewska, H. & Wierzbowski, A. 1982: The Janusfjellet Formation (Jurassic–Lower Cretaceous) at Myklegardfjellet, East Spitsbergen. *Paleontologia Polonica 43*, 107–140.

Boetius A., Ravenshlag, K., Schubert C.J., Rickert, D., Widdel, F., Gieseke, A., Amann, R., Jørgensen, B.B., Witte, U. & Pfannkuche, O. 2000: A marine microbial consortium apparently mediating anaerobic oxidation of methane. *Nature 407*, 623-626.

Bøe, R., Rise, L. & Ottesen, D. 1998: Elongate depressions on the

southern slope of the Norwegian Trench (Skagerrak): morphology and evolution. M*arine Geology 146*, 191-203.

Bromley, R.G. & Surlyk, F. 1973: Borings produced by brachiopod pedicles, fossil and Recent. *Lethaia 6*, 349-365.

Brönnimann, P. 1972: Remarks on the classification of fossil anomuran coprolites. *Paläontologishe Zeitschrift 46*, 99-103.

Campbell, K.A. 1992: Recognition of a Mio-Pliocene cold seep setting from the Northeast Pacific convergent margin, Washington, U.S.A. *Palaios 7*, 422-433.

Campbell, K.A. 2006: Hydrocarbon seep and hydrothermal vent paleoenvironments and paleontology: Past developments and future research directions. *Palaeogeography, Palaeoclimatology, Palaeoecology 232*, 362-407.

Campbell, K.A., Farmer, J.D. & Des Marais, D. 2002: Ancient hydrocarbon seeps from the Mesozoic convergent margin of California: carbonate geochemistry, fluids and palaeoenvironments. *Geofluids 2*, 63-94.

Clari, P.A., Gagliardi, C., Governa, M.E., Ricci, B. and Zuppi, G.M., 1988: I calcari di Marmorito: una testimonianza di processi diagenetici in presenza di metano. *Bollettino del Museo Regionale di Scienze Naturali Torino 5*, 197-216 (in Italian).

Conde, J.E., Diaz, U. & Sambrano, A. 1991: Disintegration of holothurian fecal pellets in beds of the seagrass Thalassia testudinum. *Journal of Coastal Research 7*, 853-862.

Conti, S. & Fontana. D. 2005: Anatomy of seep-carbonates: Ancient examples from the Miocene of the northern Appenines (Italy). *Palaeogeography, Palaeoclimatology, Palaeoecology 227*, 156-175.

Cox, L.R. 1960: The preservation of moulds of the intestine in fossil *Nuculana* (Lamellibranchia) from the Lias of England. *Palaeontology 2*, 262-269.

Dallmann, W.K., Major, H., Haremo, P., Andresen, A., Kjærnet, T. & Nøttvedt, A. 2001: Geological map of Svalbard 1:100,000, sheet C9G Adventdalen. With explanatory text. *Norsk Polarinstitutt Temakart 31/32*, 4-55.

De Boever, E., Birgel, D., Munchez, P., Peckmann, J., Dimitrov, L. & Swennen, R. 2011: Fabric and formation of grapestone concretions within an ancient methane seep system (Eocene, Bulgaria). *Terra Nova 23*, 56-61.

Dela Pierre, F., Martire, L., Natalicchio, M., Clari, P. & Petrea, C. 2010: Authigenic carbonates in Upper Miocene sediments of the Tertiary Piedmont Basin (NW Italy): Vestiges of an ancient gas hydrate stability zone? *GSA Bulletin 122*, 994-1010.

Dunham, R.J. 1962: Classification of carbonate rocks according to depositional texture. *In* Ham, W. E. (ed.): Classification of carbonate rocks: a symposium. *AAPG Memoir 1*, 108-121.

Dypvik, H., Nagy, J., Eikeland, T.A., Backer-Owe, K., Andresen, A., Haremo, P., Bjærke, T., Johansen, H. & Elverhøi, A. 1991a: The Janusfjellet Subgroup (Bathonian to Hauterivian) on central Spitsbergen: a revised lithostratigraphy. *Polar Research 9*, 21-43.

Dypvik, H., Nagy, J., Eikland, T.A., Backer-Owe, K. & Johansen, H. 1991b: Depositional conditions of the Bathonian to Hauterivian Janusfjellet Subgroup, Spitsbergen. *Sedimentary Geology 72*, 55-78.

Dypvik, H., Nagy, J. & Krinsley, D.H. 1992: Origin of the Myklegardfjellet Bed, a basal Cretaceous marker on Spitsbergen. *Polar Research 11*, 21-31.

Dypvik, H., Håkansson, E. & Heinberg, C. 2002: Jurassic-Cretaceous palaeogeography and stratigraphic comparisons in the North Greenland-Svalbard region. *Polar Research 21*, 91-108.

Dypvik, H., Mørk, A., Smelror, M., Sandbakken, P.T., Tsikalas, F., Vigran, J.O., Bremer, G.M.A, Nagy, J., Gabrielsen, R.H., Faleide, J.I., Bahiru, G.M. & Weiss, H.M. 2004: Impact breccia and ejecta from the Mjølnir crater in the Barents Sea – the Ragnarok Formation and Sindre Bed. *Norwegian Journal of Geology 84*, 143-167.

Embry, A.F. & Klovan, J.E. 1971: A Late Devonian reef tract on Northeastern Banks Island, NWT. *Canadian Petroleum Geology Bulletin 19*, 730-781.

Fauchald, K. & Jumars, P.A. 1979: The diet of worms: a study of polychaete feeding guilds. Oceanography and Marine Biology: *An Annual Review 17*, 193-284.

Feng, D. & Roberts, H.H. 2010: Initial results of comparing cold-seep carbonates from mussel- and tubeworm-associated environments at Altwater Valley lease block 340, northern Gulf of Mexico. *Deep Sea Research II 57*, 2030-2039.

Flügel, E. & Steiger, T. 1981: An Upper Jurassic sponge-algal buildup from the northern Frankenalb, West Germany. *SEPM Special Publication 30*, 371-397.

Flügel, E & Flügel-Kahler, E. 1992: Phanerozoic reef evolution: Basic questions and a data base. *Facies 26*, 167-278.

Flügel, E. 2004: *Microfacies of carbonate rocks. Analysis, Interpretation and Applicatio*n. Springer Verlag, Berlin Heidelberg, 976 pp.

Folk, R. L. 1959: Practical petrographic classification of limestones. *AAPG Bulletin 43*, 1-38.

Friedman, G.M. 1959: Identification of carbonate minerals by staining methods. *Journal of Sedimentary Research 29*, 87-97.

Gaillard, C., Rio, M., Rolin, Y. & Roux, M. 1992: Fossil chemosynthetic communities related to vents or seeps in sedimentary basins: The pseudobioherms of Southeastern France compared to other world examples. *Palaios 7*, 451-465.

Gaillard, C., Néraudeau, D. & Thierry, J. 2011: *Tithonia oxfordiana*, a new irregular echinoid associated with Jurassic seep deposits in south-east France. *Palaeontology 54*, 735-752.

Gąsiewicz, A. 1984: Eccentric ooids. *Neues Jahrbuch für Geologie und Paläontologie Monatshefte*, 204-211.

Glaub, I. 1994: Mikrobohrspuren in ausgewählten Ablagerungsräumen des europäischen Jura und der Unterkreide (Klassifikation und Palökologie). *Courier Forschungsinstitut Senckenberg 174*, 1-324.

Glaub, I. & Bundschuh, M. 1997: Comparative studies on Silurian and Jurassic/Lower Cretaceous microborings. *Courier Forschungsinstitut Senckenberg 201*, 123-135.

Goedert, J.L., Thiel, V., Schmale, O., Rau, W.W., Michaelis, W. & Peckmann, J. 2003: The Late Eocene "Whiskey Creek" methane-seep deposit (Western Washington State). Part I: Geology, palaeontology and molecular geobiology. *Facies 48*, 223-240.

Greinert, J., Bohrmann, G. & Suess, E. 2001: Gas hydrate-associated carbonates and methane-venting at Hydrate Ridge: Classification, distribution and origin of authigenic lithologies. *In* Paull, C.K. & Dillon, P.W. (eds.): Natural Gas Hydrates: Occurrence, Distribution and Detection. *Geophysical Monograph 124*, 99-113.

Greinert, J., Bohrmann, G. & Elvert, M. 2002: Stromatolitic fabric of authigenic carbonate crusts: result of anaerobic methane oxidation at cold seeps in 4,850 m water depth. *International Journal of Earth Sciences 91*, 698-711.

Haas, A., Little, C.T.S., Sahling, H., Bohrmann, G., Himmler, T. & Peckmann, J. 2009: Mineralization of vestimentiferan tubes at methane seeps on Congo deep-sea fan. *Deep-Sea Research I 5*6, 283-293.

Haas, A., Peckmann, J., Elvert, M., Sahling, H. & Bohrmann, G. 2010: Patterns of carbonate authigenesis at the Kouilou pockmarks on the Congo deep-sea fan. *Marine Geology 268*, 129-136.

Hammer, Ø., Nakrem, H.A., Little, C.T.S., Hryniewicz, K., Sandy, M.R., Hurum, J.H., Druckenmiller, P., Knutsen, E.M. & Høyberget, M. 2011: Hydrocarbon seeps from close to the Jurassic-Cretaceous boundary. *Palaeogeography, Palaeoclimatology, Palaeoecology 306*, 15-26.

Hammer, Ø. & Webb, K. 2010: Piston coring of Inner Oslofjord pockmarks: constraints on age and mechanism. *Norwegian Journal of Geology 90*, 79-91.

Hammer, Ø., Webb, K.E. & Depreiter, D. 2009: Numerical simulation of upwelling currents in pockmarks, and data from the Inner Oslofjord, Norway. *Geo-Marine Letters 29*, 269-275.

Hammes, U. 1995: Initiation and development of small-scale sponge mud-mounds, late Jurassic, southern Franconian Alb, Germany. *In* Monty, C.L.V., Bosence, D.W.J., Bridges, P.H. & Pratt, B.R. (eds.): Carbonate Mud-Mounds. Their origin and evolution. *Special Publications of The International Association of Sedimentologists 23*, 335-357.

Himmler, T., Freiwald, A., Stollhofen, H. & Peckmann, J. 2008: Late Carboniferous hydrocarbon-seep carbonates from the glaciomarine Dwyka Group, southern Namibia. *Palaeogeography, Palaeoclimatology, Palaeoecology 257*, 185-197.

Hjálmarsdóttir, H.R., Nakrem, H.A. & Nagy, J. (2012). Foraminifera from Late Jurassic – Early Cretaceous hydrocarbon seep carbonates, central Spitsbergen, Svalbard – preliminary results. *Norwegian Journal of Geology 92 (2-3)*, 157-165.

Hovland, M. 1992. Hydrocarbon seeps in northern marine waters - their occurrence and effects. *Palaios 7*, 376-382.

Hovland, M. 2002: On the self-sealing nature of marine seeps. *Continental Shelf Research 22*, 2387-2394.

Hovland, M., Talbot, M.R., Qvale, H, Olaussen, S. & Aasberg, L. 1987: Methane-related carbonate cements in pockmarks of the North Sea. *Journal of Sedimentary Petrology 57*, 881-892.

Jenkins, R.G., Kaim, A., Hikida, Y. & Tanabe, K. 2007: Methane-flux dependent lateral faunal changes in a Late Cretaceous chemosymbiotic assemblage from the Nakagawa area of Hokkaido, Japan. *Geobiology 5*, 127-139.

Jenkins, R.G., Hikida, Y., Chikaraishi, Y., Ohkouchi, N. & Tanabe, K. 2008: Microbially induced formation of ooid-like coated grains in the Late Cretaceous methane-seep deposits of the Nakagawa area, Hokkaido, northern Japan. *Island Arc 17*, 261-269.

Jørgensen, N.O. 1976: Recent high magnesian calcite aragonite cementation of beach and submarine sediments from Denmark. *Journal of Sedimentary Petrology 46*, 940-950.

Judd, A.G. & Hovland, M. 2007: S*eabed fluid flow. The Impact on Geology, Biology and the Marine Environment*. 475 pp. Cambridge University Press, Cambridge.

Kelly, S.R.A., Ditchfield, P.W., Doubleday, P.A. & Marshall, J.D. 1995: An Upper Jurassic methane-seep limestone from the Fossil Bluff Group forearc basin of Alexander Island, Antarctica. *Journal of Sedimentary Research A65*, 274-282.

Kiel, S. & Peckmann, J. 2008: Paleoecology and evolutionary significance of an Early Cretaceous *Peregrinella*-dominated hydrocarbon-seep deposit on the Crimean Peninsula. *Palaios 23*, 751-759.

Kier, P.M. 1972: Upper Miocene echinoids from the Yorktown Formation of Virginia and their environmental significance, *Smithsonian Contributions to Paleobiology 13*, 1-21.

Kobluk, D.R. & Risk, M.J. 1977: Micritization and carbonate-grain binding by endolithic algae. *Bulletin of American Association of Petroleum Geologists 61*, 1069-1082.

Krautter, M. 1997: Aspekte zur Paläökologie postpaläozoischer Kieselschwämme. *Profil 11*, 199-324.

Laubenfels, M.W. de 1955: Porifera. *In* Moore, R.C. (ed.): *Treatise on Invertebrate Paleontology. Part E. Archaeocyatha and Porifera*. 122 pp. University of Kansas Press, Lawrence.

Leinfelder, R.R., Krautter, M., Nose, M., Ramalho, M.M. & Werner, W. 1993: Siliceous sponge facies from the upper Jurassic of Portugal. *Neues Jahrbuch Geologie und Paläontologie Abhandlungen 189*, 199-254.

Levin, L.A. 2005: Ecology of cold seep sediments: interactions of fauna with flow, chemistry and microbes. *Oceanography and Marine Biology: An Annual Review 43*, 1-46.

Leys, S.P., Mackie, G.O. & Reiswig, H.M. 2007: The biology of glass sponges. A*dvances in Marine Biology 52*, 1-145.

Martens, C.S., Chanton, J.P. & Paull, C.K. 1991: Biogenic methane from abyssal brine seeps at the base of the Florida escarpment. *Geology 19*, 851-854.

Monty, C.L.V., Bosence, D.W.J., Bridges, P.H. & Pratt, B.R. (eds.) 1995: Carbonate Mud-Mounds: Their Origin and Evolution. *Special Publication of the International Association of Sedimentologists 23*. 537 pp. Blackwell, Oxford.

Naehr, T.H., Rodriguez, N.M, Bohrmann, G., Paull, C.K. & Botz, R. 2000: Methane-derived authigenic carbonates associated with gas hydrate decomposition and fluid venting above the Blake Ridge diapir. *Proceedings of the Ocean Drilling Program, Scientific Results 164*, 285-300.

Nagy, J. & Basov, V.A. 1998: Revised foraminiferal taxa and biostratigraphy of Bathonian to Ryazanian deposits in Spitsbergen. *Micropaleonotology 44*, 217-255.

Nagy, J., Løfaldli, M. & Bäckström, S.A. 1988: Aspects of foraminiferal distribution and depositional conditions in Middle Jurassic to Early Cretaceous shales in eastern Spitsbergen. *Abhandlungen der Geologischen Bundesanstalt Wien 30*, 287–300.

Neuweiler, F., Daoust, I., Bourque, P.A. & Burdige, D.J. 2007: Degradative calcification of modern siliceous sponge from the Great Bahama Bank, The Bahamas: A guide for interpretation of ancient sponge-bearing limestones. *Journal of Sedimentary Research 77*, 552-563.

Ogg, J., Hinnov, L. & Huang, C. 2012: Jurassic. *In:* Gradstein, F.M., Ogg, J.G., Schmitz, M.A., Ogg, G. (Eds.): *The Geologic Time Scale 2012. Volume 2*. Elsevier Publishing Press, 731-791.

Olóriz, F., Reolid, M., Rodríguez-Tovar, F.J., 2003: A Late Jurassic carbonate ramp colonized by sponges and benthic microbial communities (External Prebetic, southern Spain). *Palaios 18*, 528-545.

Olu-Le Roy, K., Sibuet, M., Fiala-Medioni, A., Gofas, S., Salas, C., Mariotti, A., Foucher, J.P. & Woodside, J. 2004: Cold seep communities in the deep eastern Mediterranean Sea: composition, symbiosis and spatial distribution on mud volcanoes. *Deep-Sea Research I 51*, 1915-1936.

Paull, C.K., Hecker, B., Commeau, R., Freeman-Lynde, R.P., Neumann, C., Corso, W.P., Golubic, S., Hook, J.E., Sikes, E. & Curray, J. 1984: Biological communities at the Florida Escarpment resemble hydrothermal vent taxa. *Science 226*, 965-967.

Peckmann, J. & Thiel, V. 2004: Carbon cycling at ancient methane-seeps. *Chemical Geology 205*, 443-467.

Peckmann, J., Goedert, J.L., Thiel, V., Michaelis, W. & Reitner, J. 2002: A comprehensive approach to the study of methane-seep deposits from the Lincoln Creek Formation, western Washington State, USA. *Sedimentology 49*, 855-873.

Peckmann, J., Little, C.T.S., Gill, F. & Reitner, J. 2005: Worm tube fossils from the Hollard Mound hydrocarbon-seep deposits, Middle Devonian, Morocco: Palaeozoic seep-related vestimentiferans? *Palaeogeography, Palaeoclimatology, Palaeoecology 227*, 242-257.

Peckmann, J., Senowbari-Daryan, B., Birgel, D & Goedert. J. 2007: The crustacean ichnofossil *Palaxius* associated with callianassid body fossils in an Eocene methane-seep limestone, Humtulips Formation, Olympic Peninsula, Washington. *Lethaia 40*, 273-280.

Peckmann, J., Kiel, S., Sandy, M.R., Taylor, D.G. & Goedert, J.L. 2011: Mass occurrences of the brachiopod *Halorella* in Late Triassic methane-seep deposits, Eastern Oregon. *Journal of Geology 119*, 207-220.

Pemberton, G.S., Jones, B. & Edgecombe, G. 1988: The influence of Trypanites in the diagenesis of Devonian stromatoporoids. *Journal of Palaeontology 62*, 21-32.

Peryt, T.M. (Ed.) 1983: *Coated grains*. 655 pp. Berlin, Springer.

Pickerill, R.K. & Harland, T.L. 1984: Middle Ordovician microborings of probable sponge origin from Eastern Canada and Southern Norway. *Journal of Paleontology 58*, 885-891.

Pisera, A. 1997: Upper Jurassic siliceous sponges from the Swabian Alb: taxonomy and paleoecology. *Palaeontologia Polonica 57*, 1-137.

Pratt, B.R, Raviolo, M.M. & Osvaldo, B.L. 2012: Carbonate platform dominated by peloidal sands: Lower Ordovician La Silla Formation of the eastern Precordillera, San Juan, Argentina. *Sedimentology 59*, 843-866.

Radtke, G. 1991: Die mikroendolithischen Spurenfossilien im Alt-Tertiär West-Europas und ihre palökologische Bedeutung. *Courier Forschungsinstitut Senckenberg 138*, 1-185.

Reid, R.P. & Macintyre, I.G. 2000: Microboring versus recrystallization: further insight into the micritization process. *Journal of Sedimentary Research 70*, 24-28.

Reid, R.P., MacIntyre, I.G. & Post, J.E. 1992: Micritized skeletal grains in northern Belize lagoon: a major source of Mg-calcite mud. *Journal of Sedimentary Petrology 62*, 145-156.

Reitner, J. 1993: Modern cryptic microbialite/metazoan facies from

Lizard Island (Great Barrier Reef, Australia). Formation and concepts. Facies 29, 3-40.

Reitner, J. & Schumann-Kindel, G. (1997). Pyrite in mineralized sponge tissue: product of sulfate reducing sponge related bacteria? *Facies 36*, 272-276.

Reitner, J., Peckmann, J., Reimer, A., Schumann, G. & Theil, V. 2005: Methane-derived carbonate build-ups and associated microbial communities at cold seeps on the lower Crimean shelf (Black Sea). *Facies 51*, 66-79.

Reolid, M., Nagy, J., Rodríguez-Tovar, F.J. & Olóriz, F. 2008: Foraminiferal assemblages as palaeoenvironmental biocindicators in Late Jurassic epicontinental platforms: Relation with trophic conditions. *Acta Palaeontologica Polonica 53*, 705-722.

Reolid, M., Nagy, J., Rodríguez-Tovar, F.J., 2010. Ecostratigraphic trends of Jurassic agglutinated foraminiferal assemblages as a response to sea-level changes in shelf deposits of Svalbard (Norway). *Palaeogeography Palaeoclimatology Palaeoecology 293*, 184-196.

Rigby, J.K. & Goedert, J.L. 1996: Fossil sponges from a localized cold-seep limestone in Oligocene rocks of the Olympic Peninsula, Washington. *Journal of Paleontology 70*, 900-908.

Rousseau, J. & Nakrem, H.A. 2012: An Upper Jurassic Boreal echinoderm Lagerstätte from Janusfjellet, central Spitsbergen. *Norwegian Journal of Geology Vol 92*, 133-148.

Sahling, H., Rickert, D., Lee, R.W., Linke, P. & Suess, E. 2002: Macrofaunal community structure and sulfide flux at gas hydrate deposits from the Cascadia convergent margin, NE Pacific. *Marine Ecology Progress Series 231*, 121–138

Samankassou, E., Tresch, J. & Strasser, A. 2005: Origin of peloids in Early Cretaceous deposits, Dorset, South England. *Facies 51*, 264-273.

Sassen, R., Joye, S., Sweet, S.T., DeFreitas, D.A., Milkov, A.V. & MacDonald, I.R. 1999: Thermogenic gas hydrates and hydrocarbon gases in complex chemosynthetic communities, Gulf of Mexico continental slope. *Organic Geochemistry 30*, 485-497.

Senowbari-Daryan, B., Gaillard, C. & Peckmann, J. 2007: Crustacean microcoprolites from Jurassic (Oxfordian) hydrocarbon-seep deposits of Beauvoisin, southeastern France. *Facies 53*, 229-238.

Senowbari-Daryan, B., Zühlke, R., Bechstädt, T. & Flügel, E. 1993: Anisian (Middle Triassic) buildups of the Northern Dolomites (Italy): the recovery of reef communities after the Permian/Triassic crisis. *Facies 28*, 181-256.

Sibuet, M. & Olu, K. 1998: Biogeography, biodiversity and fluid dependence of deep-sea cold-seep communities at active and passive margins. *Deep Sea Research II 45*, 517-567.

Skompski, S. & Szulczewski, M. 1994: Tide-dominated Middle Devonian sequence from the northern part of the Holy Cross Mountains (Central Poland). *Facies 30*, 247-266.

Strasser, A. 1986: Ooids from the Purbeck limestones (lowermost Cretaceous) of the Swiss and French Jura. *Sedimentology 33*, 711-727.

Temara, A., de Ridder, C., Kuenen, J.G. & Robertson, L.A. 1993: Sulfide-oxidizing bacteria in the burrowing echinoid, *Echinochardium cordatum (*Echinodermata*). Marine Biology 115*, 179–185.

Trammer, J. 1989: Middle to Upper Oxfordian sponges of the Polish Jura. *Acta Geologica Polonica 39*, 49-91.

Tsunogai, U., Yoshida, N. & Gamo, T. 2002: Carbon isotopic evidence of methane oxidation through sulfate reduction in sediment beneath cold seep vents on the seafloor at Nankai Trough. *Marine Geology 187*, 145-160.

Tucker, M.E. & Wright, V.P. 1990: *Carbonate sedimentology*. Blackwell, Oxford. 482 pp.

Valentine, D.L. 2002. Biogeochemistry and microbial ecology of methane oxidation in anoxic environments: a review. *Antonie van Leeuwenhook 81*, 271-282.

Van Dover, C.L., Aharon, P., Bernhard, J.M., Caylor, E., Doerries, M., Flickinger, W., Golhooly, W., Goffredi, S.K., Knick, K.e., Macko, S.A., Rapaport, S., Raulfs, E.C., Ruppel, C., Salerno, J., Seitz, R.D., Sen Gupta, B.K., Shank, T., Turnispeed, M. & Vrijenhoeck, R.C. 2003: Blake Ridge methane seeps: characterization of a soft-sediment, chemosynthetically based ecosystem. *Deep-Sea Research I*, 281-300.

Vaughn Barrie, J., Cook, S. & Conway, K.W. 2011: Cold seeps and benthic habitat on the Pacific margin of Canada. *Continental Shelf Research 31*, S85-S92.

Vogel, K. & Marincovich Jr., L. 2004: Paleobathymetric implications of microborings in Tertiary strata of Alaska, USA: *Palaeogeography, Palaeoclimatology, Palaeoecology 206*, 1-20.

Vogel, K. & Brett, C.E. 2009: Record of microendoliths in different facies of the Upper Ordovician in the Cincinnati Arch region USA: The early history of light-related microendolithic zonation. *Palaeogeography, Palaeoclimatology, Palaeoecology 281*, 1-24.

Voigt, E. 1975: Tunnelbaue rezenter und fossiler Phoronidea. *Paläontologishe Zeitschrift 49*, 135-167.

Warnke, K. 1995: Calcification processes of siliceous sponges in Viséan limestones (Counties Sligo and Leitrim, Northwestern Ireland). *Facies 33*, 215-228.

Wendt, J. & Aigner, T. 1985: Facies patterns and depositional environments of palaeozoic cephalopod limestones. *Sedimentary Geology 44*, 263-300.

Wendt, J. & Belka, Z. 1991: Age and depositional evironment of Upper Devonian (Early Frasnian to Early Fammenian) black shales and limestones (Kellwasser Facies) in the Eastern Anti-Atlas, Morocco. *Facies 25*, 51-90.

Wierzbowski, A., Hryniewicz, K., Hammer, Ø, Nakrem, H.A. & Little, C.T.S. 2011: Ammonites from hydrocarbon seep carbonate bodies from the uppermost Jurassic – lowermost Cretaceous of Spitsbergen and biostratigraphical importance. *Neues Jahrbuch für Geologie und Paläontologie Abhandlungen 262/3*, 267-288.

Winland, H.D. 1968: The role of high Mg-calcite in the preservation of micrite envelopes and textural features of aragonite sediments. *Journal of Sedimentary Petrology 38*, 1320-1325.

Zardus, J.D. 2002: Protobranch bivalves. *Advances in Marine Biology 42*, 1-65.